Module 6

Lecture 1

Shear Strength

Stability of many geotechnical engineering problems is associated with the measurement, analysis, and prediction of shear strength of the soils in their natural state. Geotechnical engineering problems such as bearing capacity of foundations, stability of natural & man-made soil slopes, design of pavements, and earth retaining problems require the qualitative and quantitative prediction of the strength. The shear strength of the soil may be defined as the maximum resistance along the failure plane in soils per unit cross-sectional area under the load application. It was well understood that the strength of the soil is related to stress state in the soil. The state of stress in a soil consists of certain combination of stress variables that are independent of material properties. They are called stress-state variables. Stress-state variables are required for the characterization of the stress conditions in the soil. The number of stress state variables to describe the stress state of soil depends on the degree of saturation. The effective stress is a sole stress state variable of a saturated soil which can completely define the state of stress. Thus the mechanical behavior of saturated soils is completely controlled by the effective stress. However, ascertaining the stress state variables for unsaturated soils is very difficult. Of late, two stress-state variables viz. net normal stress and matric suction have been widely accepted and used. Some of the early developments of shear strength of soils are briefly described in the following section.

Some early developments

The early quantification and application of shear strength was done in the eighteenth century by a French scientist, Coulomb, in his classical work on friction model. This work was drawn on the work of *Leonardo da Vinci* on law of frictional materials in the sixteenth century. Coulomb described useful design models based on his work that are used even today in the design of retaining walls and other applications that are central to the geotechnical engineering.

Coulomb distinguishes soil and rock only based on its relative strength. The soil was considered to be a rigid homogeneous material similar to rock mass. This one-phase material ruptures into two different blocks at failure. Based on his experiments on solid rock samples, Coulomb hypothesized that these blocks slide on each other along the slip surfaces. The state of soil at peak stress was described in his classical work. It was suggested that both cohesion and friction need to be overcome along the slip surface during the shearing as described in the following classical friction model

$$\tau = c + \sigma \tan\phi \qquad (6.1)$$

where τ is the shear strength; σ the normal stress component across the slip surface; c and ϕ are cohesion and angle of internal friction that are the mathematical constants defining a linear relationship between τ and σ. However, Terzaghi's perception of the soil as a two-phase system in 1920 has brought the effective stress principle which is described as $\sigma' = \sigma - u_w$, where u_w is the neutral stress or positive pore water pressure.

Based on his effective stress principle, it was demonstrated that shear stresses in the soil can only be resisted by the solid particles. Thus, the shear strength should be expressed as a function of effective normal stress at failure as

$$\tau_f = c' + \sigma'_f \tan\phi' \qquad (6.2)$$

in which the effective stresses are used in place of total normal stresses. The dash over τ is not used as water does not contribute to shear. Equation (6.2) describes that the failure occurs at any given point in the soil mass under the application of a critical combination of shear and effective normal stresses. The stress state in soil is conveniently represented by Mohr's circle defined by the effective principal stresses as shown in Fig. 6.1. The line drawn tangent to all the Mohr's circles at failure is the failure envelope given in Fig. 6.1. A state of stress represented by stress points above the failure envelope do not exist. On the other hand, if the state of stress of a soil locatesd entirely below the failure envelope, the shear strength of the soil is not exceeded and the soil mass is stable. The shear stresses along the failure envelope describe the shear strength of the soil under the respective effective normal stresses. The envelope passes through origin when the cohesion intercept is zero, which is the case of sands.

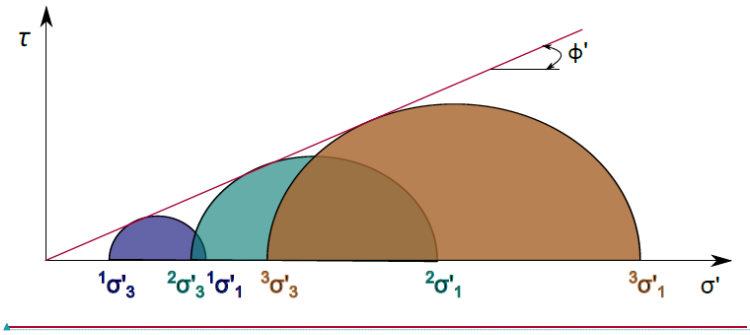

Fig. 6.1. State of stresses at failure and Mohr-Coulomb (M-C) failure envelope in saturated soils

The relation between effective principle stresses and the shear strength parameters can be obtained using the Mohr's circle shown in Fig. 6.2.

Formatted: Font: 12 pt, Font color: Text 1, Complex Script Font: 12 pt

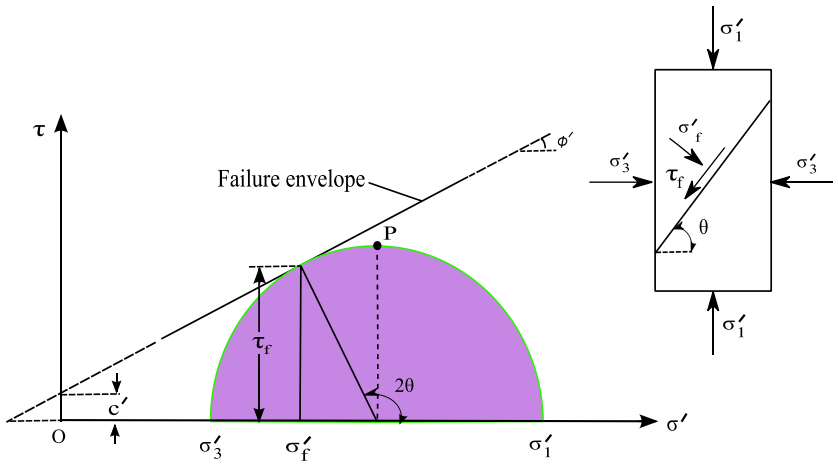

Fig. 6.2 Mohr-Coulomb's failure criterion

The relationship may be written as

$$\sigma_1' = \sigma_3' \tan^2\left(45^0 + \frac{\phi'}{2}\right) + 2c' \tan\left(45^0 + \frac{\phi'}{2}\right) \qquad (6.3)$$

which is referred to as Mohr-Coulomb failure criterion.

The aforementioned shear strength parameters are often determined in the laboratory using direct shear and triaxial test apparatus on representative soil samples obtained from the field. The testing procedure is summarized briefly here.

Direct shear is a simple test conducted routinely in the geotechnical engineering laboratory. The soil sample is confined in a square split metal box. The metal box can split into two halves at mid-height during the application of shear as shown in Fig. 6.3.

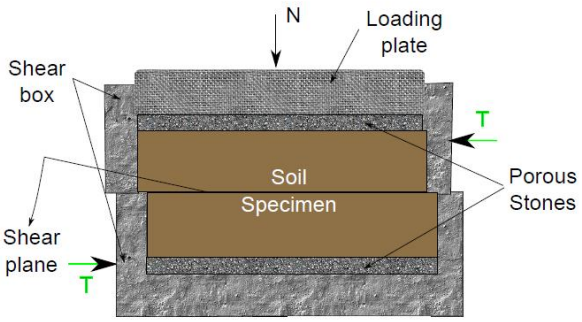

Fig. 6.3. Free-body diagram of direct shear apparatus

Formatted: Font: 12 pt, Font color: Text 1, Complex Script Font: 12 pt

A vertical normal load (N) is applied to the specimen and shear load (T) is applied on horizontal plane of one half either at constant strain or constant stress condition. The applied shear makes the two halves to move relatively along the pre-determined failure plane under the vertical normal load. The displacements in horizontal and vertical directions are measured, during the test, using dial gauges mounted on the sample along vertical and horizontal directions. The test is stopped when either peak strength or maximum displacement is observed. The tests are conducted using similar samples under different vertical normal loads. The shear strength parameters are obtained from the failure envelope which can be obtained by plotting the shear stresses at failure against the normal stress for each test as shown in Fig. 6.4.

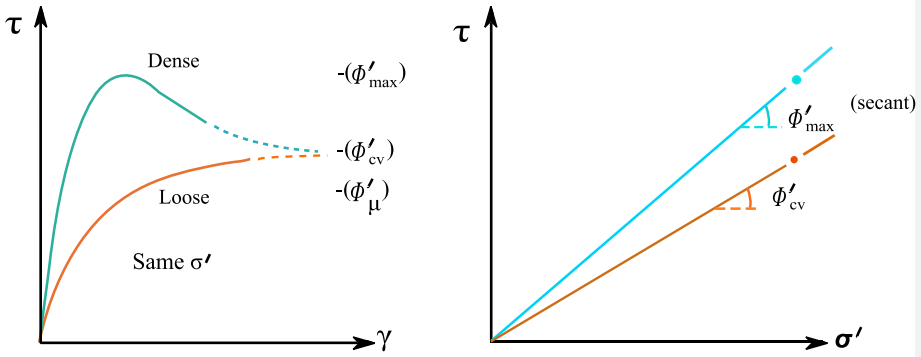

Fig. 6.4. Shear envelopes obtained by direct shear tests (a) shear stress vs. shear strain plot (b) shear stress at failure vs. normal stress

Triaxial test is a most widely used test in the laboratory for measuring the shear strength of soils. The drainage can be controlled advantageously during shearing in this test. A cylindrical sample is contained in a Perspex cell as shown in Fig. 6.5a-b. Connections to the soil sample from the external water reservoir are established to control the pore water pressure in the soils and to provide free drainage. An all-round water pressure, σ_3 , is initially applied by pressurizing the water in the cell. Consolidation is allowed during this stage, if required, depending on the test condition.

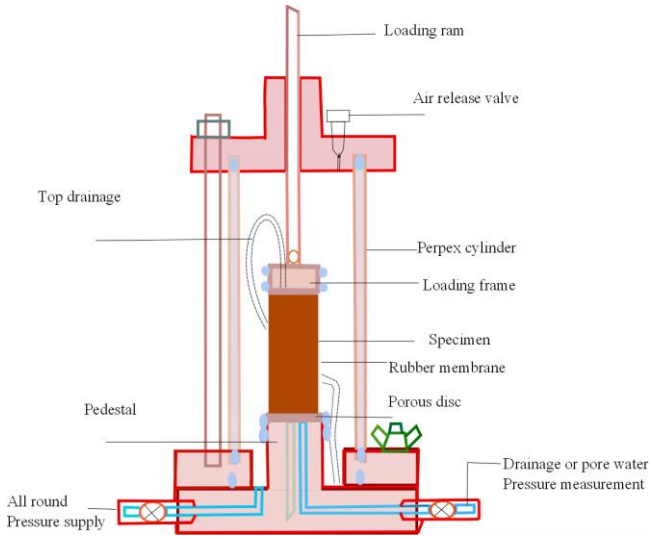

(a)

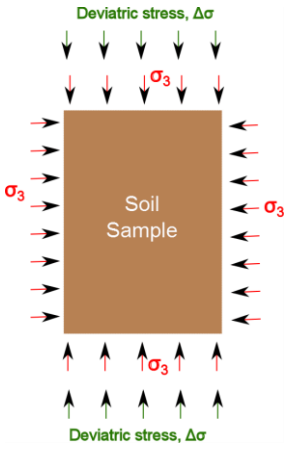

(b)

Fig. 6.5. (a) Schematic of laboratory triaxial set-up (b) Stress system in soils in triaxial test

The normal load, to induce deviatric stress, is then applied to generate shear stresses in soil sample. The dissipation of excess pore water pressures can be allowed depending on the test condition. The volume change in the soil can indirectly be measured from the measurement of volume of water leaving the soil sample during the excess pore water pressure dissipation. The effective principle stresses at failure can be used to determine the shear strength parameters.

Lecture 2

Stresses in unsaturated soils

As described in the previous lecture, the macroscopic description of shear strength as a function of the stress state variable, effective stress, leads to material constants viz. cohesion and angle of internal friction. The empirical equation containing the material parameters together with the effective stress define the failure conditions of the saturated soils. As it was noted, the pore water pressure in a saturated soil is compressive and isotropic. The pore pressure in saturated soils totally contributes to decrease in the total stress according to the Terzaghi's effective stress principle. However, the pore water pressure is negative in the pores of unsaturated soils due to the solid-water-air interface effects. The behavior of unsaturated soils is highly complex due to the interfacial effects between different phases in soil. The relative amount pore water or pore air and corresponding pressures have direct bearing on the state of stress acting at particle level as shown in Fig. 6.6.

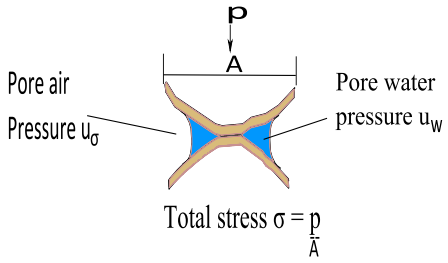

Fig. 6.6 Microscopical representation of contact pressures between different phases

The contribution of this negative pore water pressure on the total stress is less than the contribution of positive pore-water pressure in saturated soils. Terzaghi's stress state variable, therefore, can't capture the shear strength behavior of unsaturated soils for the same reason. Therefore, the stress state in unsaturated soils is more complex. A simple conceptual analysis of stress distribution in the soil is described here considering different cases to understand the effect of degree of moisture content on the stress state.

Case-I: Let us consider a homogeneous soil layer which is initially saturated due to the ground water table located at the ground surface as shown in Fig. 6.7a. Assume that the soil has a unit weight of γ.

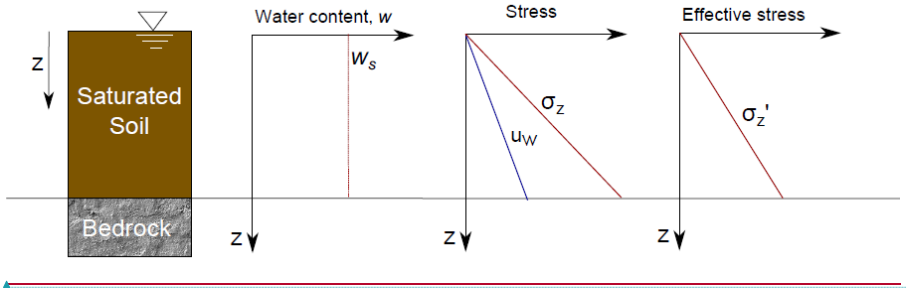

Fig. 6.7a Conceptual profiles in saturated soil (after Lu and Likos, 2004)

The total vertical stress at any given point in the soil mass due to overburden pressure is γz, where z is the depth of the point of interest from the ground surface. Similarly, the pore water pressure is given by $\gamma_w z$, where γ is the unit weight of water. The vertical effective stress profiles are obtained using Terzaghi's effective stress principle and graphically shown the linear variation with depth (Fig. 6.7a)

Case – II: Now, if the water table in the soil dips to the soil-bedrock interface suddenly, the moisture content variation in the soil varies according to pore-size distribution and stress state of that soil. Thus let us assume a moisture distribution at equilibrium above the water table varies linearly from 5% at the ground surface to 30% (fully saturated) at the water table; pore-water pressure varies from – 98 kPa at the ground surface to 0 at the ground water tabel. If we assume that the whole pore water pressure contributes to the total stress, the effective stress becomes $\sigma' = \sigma + u_w$. The consequent pore pressure profile is distributed linearly with depth. Here, the tensile pore water pressure varies from – 98 kPa at the ground surface to zero at the water table. The corresponding total stress, pore water pressure, and effective stress profiles are given in Fig. 6.7b.

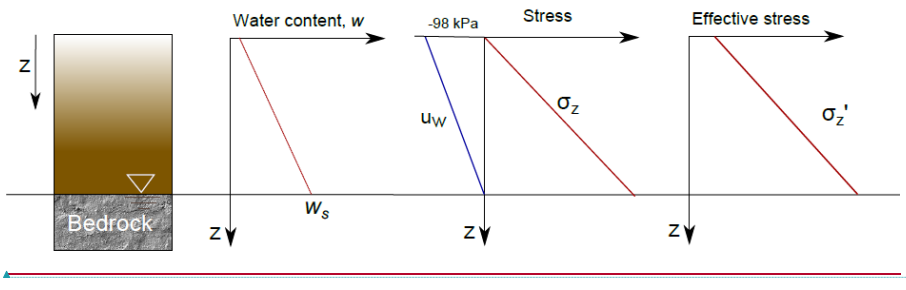

Fig. 6.7b. Conceptual profiles in unsaturated soil (after Lu and Likos, 2004)

Case – III: As mentioned before, the contribution of negative pore water pressure to the total pressure is not full, a fraction of pore pressure contribution is considered. The assumed

Formatted: Font: 12 pt, Font color: Text 1, Complex Script Font: 12 pt

Formatted: Font: 12 pt, Font color: Text 1, Complex Script Font: 12 pt

effective stress relation becomes $\sigma' = \sigma + \lambda u_w$ where λ is the effective stress parameter and its value is less than unity. The corresponding stress distribution is illustrated in **Fig 6.7c**.

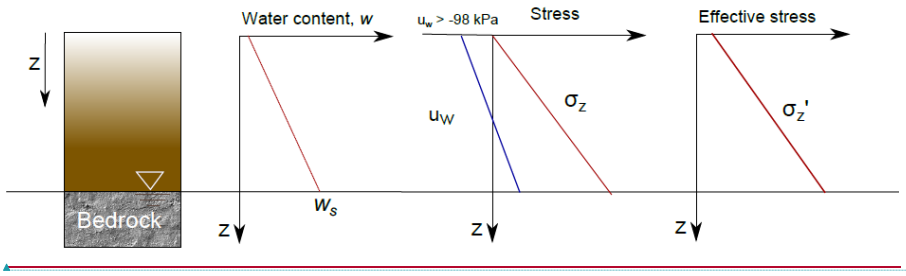

Fig. 6.7c Conceptual profiles in unsaturated soil with different representation of stresses (after Lu and Likos, 2004)

It can be seen from the above conceptual illustrations that the effective stress increases considerably due to unsaturation. The shear strength of the soil thus increases with unsaturation due to the presence of negative pore water pressure. However, it was not clear how much percentage of negative pore water pressure contributes to the increase in shear strength. Therefore, the stress state in the pore-water has a direct bearing on the macroscopic physical behavior of the unsaturated soils, viz. shear strength and volume change. The relative amount of pore fluid in the unsaturated field soils varies with time and location due to climatic conditions and natural processes. An accurate analysis of shear strength of unsaturated soils is, therefore, a fundamental requirement in all the geotechnical applications as discussed in the introduction of this web course.

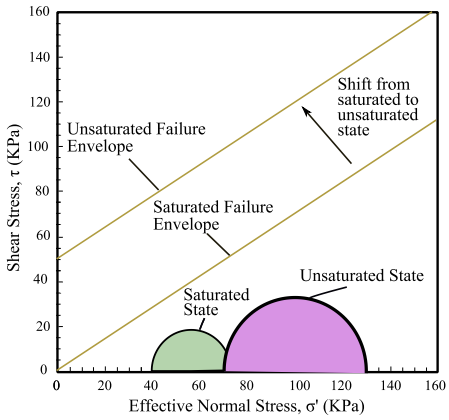

Fig. 6.8. Conceptual stress analysis of soils in saturated and unsaturated conditions (after, Lu and Likos 2004)

Some researchers came up with a more realistic approach by considering soil as a three-phase system. It consists of soil solid particles, pore water, and pore air. The state of stress

Formatted: Font: 12 pt, Font color: Text 1, Complex Script Font: 12 pt

in unsaturated soils is, therefore, vitally different from the one-phase (i.e. Coulomb's friction law) and two-phase (i.e. Terzaghi's effective stress concept) approximations for soils made earlier. Accurate description of ranges of effective stress in unsaturated soils was given by Bishop (1959) based on the extended Terzaghi's effective stress equation to explain the laboratory shear strength test results which can be written as

$$\sigma' = (\sigma - u_a) + \chi(u_a - u_w) \qquad (6.4)$$

where σ' is the effective stress, σ the total normal stress, χ the effective stress parameter, u_a the pore water pressure, and u_a the pore water pressure. The quantity $(u_a - u_w)$ is the matric suction and $(\sigma - u_a)$ is called net normal stress. The effective stress parameter is a material constant that depends on degree of saturation. The value of χ varies between 0 (dry soils) and 1 (saturated soils). The relation between χ and degree of saturation is obtained experimentally. This was the first attempt to consider two independent stress state variables for describing the shear strength of unsaturated soils.

The component of net normal stress in the equation is applicable to bulk soil while the matric suction component represents inter-particle stress due to suction. This approach describes the contribution of water-air interface in the soil pore space to the net inter-particle stress.

The measurement of shear strength of unsaturated soils is fundamentally important to understand the strength behavior theoretically. Thus, the conventional shear tests have been modified to suit the need for testing the unsaturated soils. The following lectures elaborate the details of the measurement techniques.

Lecture 3

Measurement of the shear strength

Shear strength determination of unsaturated soils in laboratory has been the subject matter in geotechnical engineering for several decades. However, the measurement and analysis of strength of field soils is highly complex. During the shearing process in the strength determination tests, the pore air pressure needs to be properly controlled for defining shear strength of the soil at any given normal and matric stresses. The measurement of total change in volume in the soil during the shear application, in conventional triaxial tests, is done through the control or measurement of pore water in the soil. The loss of pore water in a drained shear test is directly related to the volume change in the soil sample. However, measuring the volume changes of unsaturated soils during shearing process is not possible in the conventional shear tests. This is because some percentage of pore-air dissipates through the membrane walls and the remaining gets compressed to allow the volume changes in soil as illustrated in Fig. 6.9.

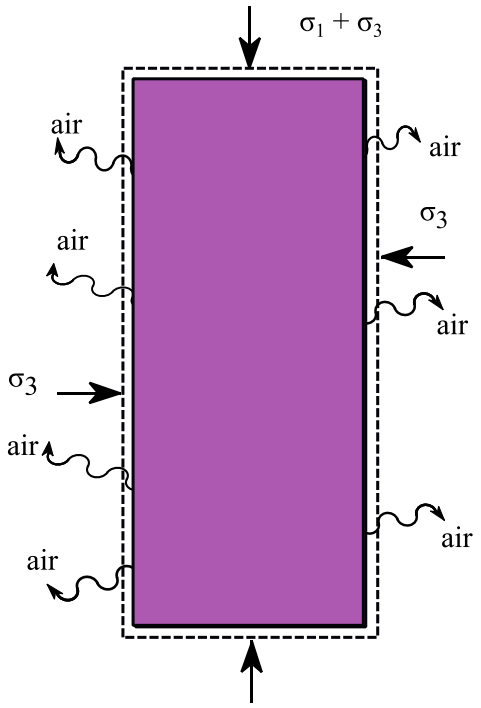

Fig. 6.9. Conceptual diagram representing the changes in the state under stresses

The conventional triaxial and shear box apparatus are modified to control the pore air pressure and matric suction during the testing process. Axis-translation technique has been successfully used to control matric suction in these modified testing devices for measuring the strength of unsaturated soil. The two measuring devices are described here.

Extended triaxial apparatus

Triaxial test is yet a favorite shear testing device for geotechnical engineers. Several test results on unsaturated triaxial testing machines have been published by Charles W. W. Ng with his research group at Hong Kong University of Science and Technology (HKUST). Two types of devices are commonly used for shear strength testing of unsaturated soils in laboratory. The difference between these devices is based on the employed technique to control the matric suction. The commonly known technique to control the suction in triaxial is axis-translation technique. Osmotic method is used as an alternative to axis-translation technique for controlling matric suction in triaxial device.

(i) Triaxial apparatus using axis-translation

The triaxial device for unsaturated soil testing consists of conventional triaxial cell, pressure controllers, transducers, total volume change measuring system, and an indicator to measure (Ng and Menzies, 2007). The pressure controllers are used for controlling triaxial cell pressure, pore air pressure, back pressure, and axial stress independently. The transducers are required for measuring axial force by internal load cell, axial displacement by LVDT, total volume change by differential pressure transducer, cell pressure, pore-water pressure, and pore air pressure. These controllers are connected to computer by an interface card. The shear strength of the soil under various stress paths and drainage conditions can be established at any given matric suction and normal stress values using the attached controllers and transducers to the conventional triaxial cell apparatus. Schematic diagram of the triaxial apparatus using axis-translation is shown in Fig 6.10. A cylindrical unsaturated soil sample is seated in good contact with HAE disk for establishing external hydraulic connection with soil pore water to the water compartment, provided at the bottom of the pedestal. The water compartment also serves as a channel for flushing trapped air bubbles due to air diffusion. As shown in Fig 6.10, coarse porous disk is placed on the top of the soil sample, i.e. between the soil sample and the top cap, for establishing external connection with soil pore air. The soil sample may be consolidated under isotropic effective confining pressure, if required. Desired matric suction is applied to the soil sample by controlling the pore water and pore-air pressures through HAE disk and coarse porous disk respectively, prior to shearing process. The established matric suction is measured at equilibrium as the difference between the applied air pressure and the pore water pressure. The required deviator stress, $(\sigma_1 - \sigma_3)$, is applied for shear testing. The deviator stress and volumetric strain under axial loading are measured using transducers under drained or undrained conditions. The samples are tested under different matric suction and net normal

stress, $(\sigma_1 - u_a)$, values to develop the failure envelope. Experimental results of triaxial stress path tests based on axis-translation technique on unsaturated soil are given in Fig 6.11.

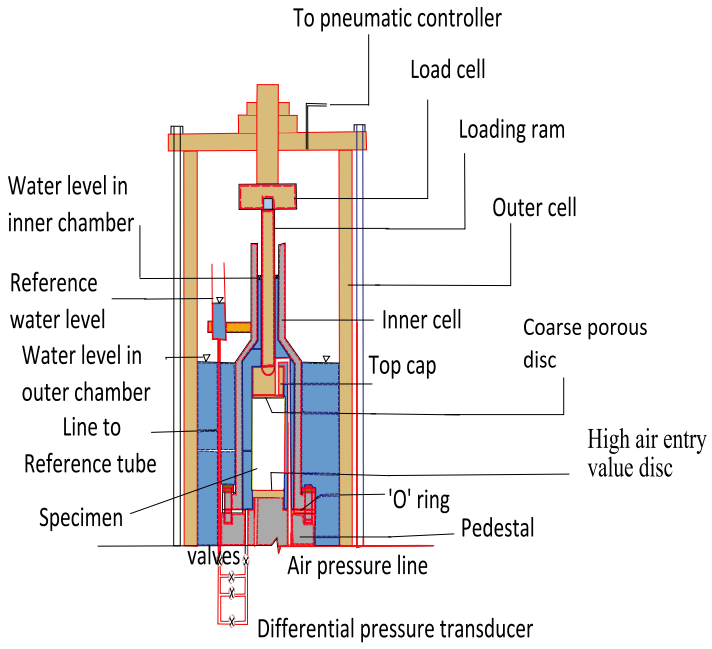

Fig. 6.10 Modified triaxial cell apparatus for testing unsaturated soils (after Ng and Chen 2005)

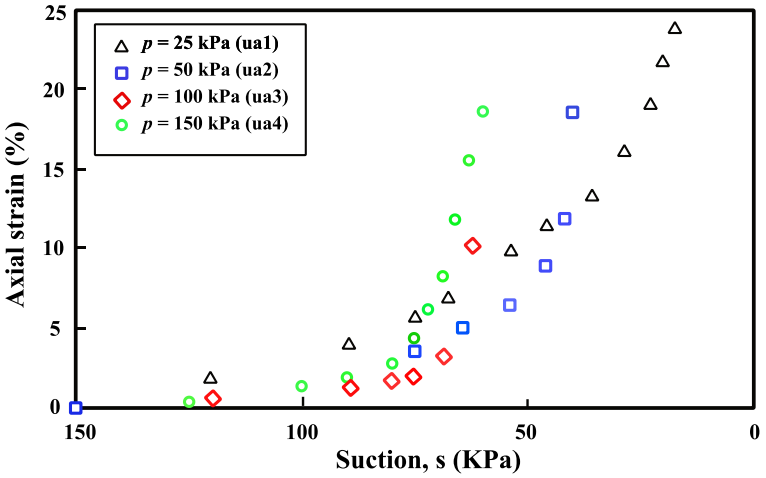
p = 25 kPa (ua1)
p = 50 kPa (ua2)
p = 100 kPa (ua3)
p = 150 kPa (ua4)
Axial strain (%)
25
20
15
10
5
0
150
100
50
0
Suction, s (KPa)

(a)

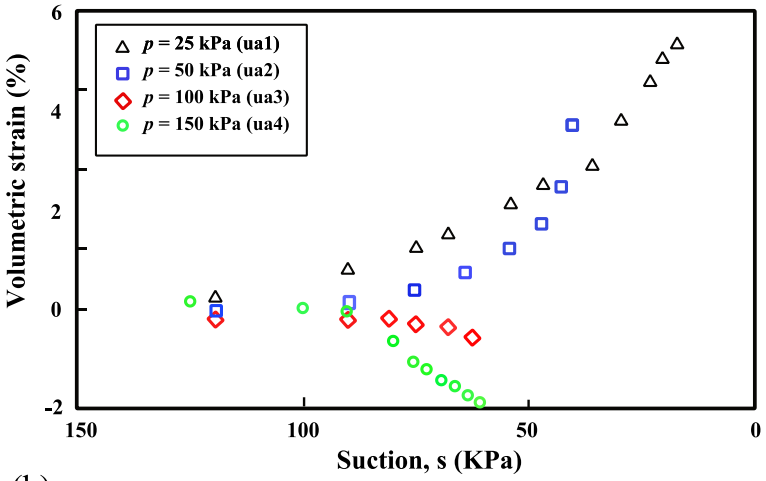
p = 25 kPa (ua1)
p = 50 kPa (ua2)
p = 100 kPa (ua3)
p = 150 kPa (ua4)
Volumetric strain (%)
6
4
2
0
-2
150
100
50
0
Suction, s (KPa)

(b)

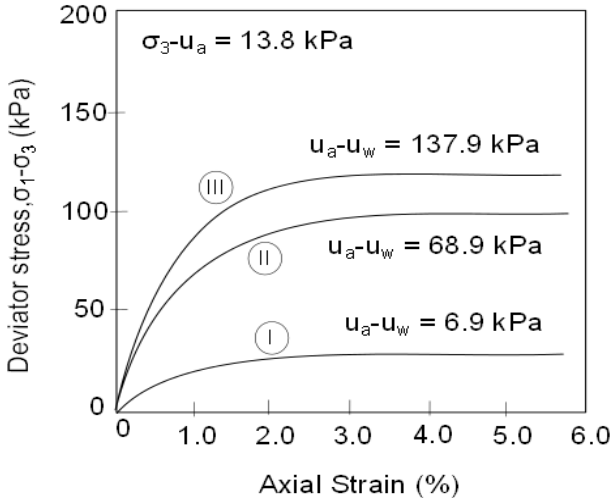

(a)

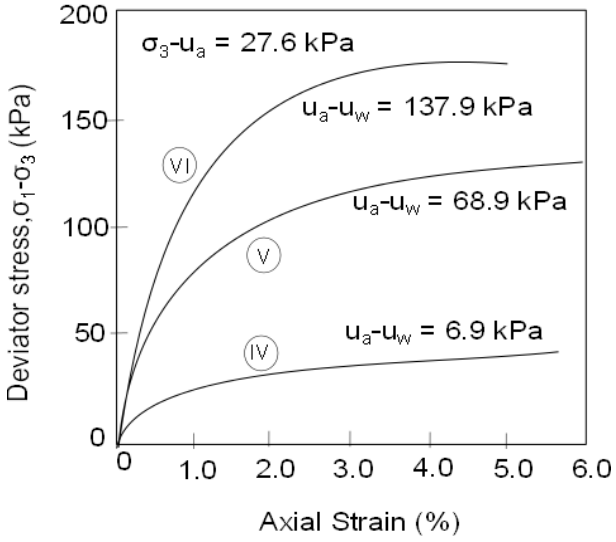

(b)

Fig. 6.11b. CD tests data on unsaturated soil using modified triaxial set-up (after Blight, 1967)

It can be observed that the maximum shear stress (yield stress) increases with matric suction for a given value of all round pressure (Fig. 6.11a). Further, the increase in all-round pressure has the same effect as the matric suction qualitatively (Fig. 6.11b). The major limitation of triaxial measuring system for strength of unsaturated soils using axis-translation technique is pertaining to the limitation on applied maximum suction value. The maximum allowable suction is limited by the maximum cell pressure and air-entry value of HAE material. Further, inaccurate results may obtain through wetting stress path near saturation due to cavitation effects. It was experimentally verified by researchers that discrepant results observed between the stress conditions on the laboratory soil samples obtained by the use of axis-translation technique in triaxial apparatus and other techniques where the pore air pressure is at the atmospheric pressure.

(ii) Triaxial apparatus using osmotic method

Osmotic technique is an alternative to the axis-translation technique to control matric suction for testing unsaturated soil strength in triaxial apparatus. Osmotic technique is gaining popularity to circumvent the problems associated with axis-translation technique. The mechanism of osmotic technique to control matric suction in unsaturated soils is already discussed earlier. The Fig 6.13 provides the schematic diagram of triaxial apparatus using osmotic method for controlling the suction. The principle of triaxial testing here is same as the previously discussed method, except the mechanism of matric suction control. A semi-permeable membrane separates the soil specimen and osmotic solution as shown in the figure. Semi-permeable membranes permeate water molecules but prevent the permeation of larger solute molecules and soil particles. It develops an osmotic suction across the membrane. The difference of osmotic suction across the membrane is equal to the difference of matric suction on both sides of membrane. The maximum applied matric suction depends on the concentration of the solute, type of solute, and performance of semi-permeable membranes. Polyethylene glycol (PEG) is the commonly used solute in geotechnical testing due to its simplicity.

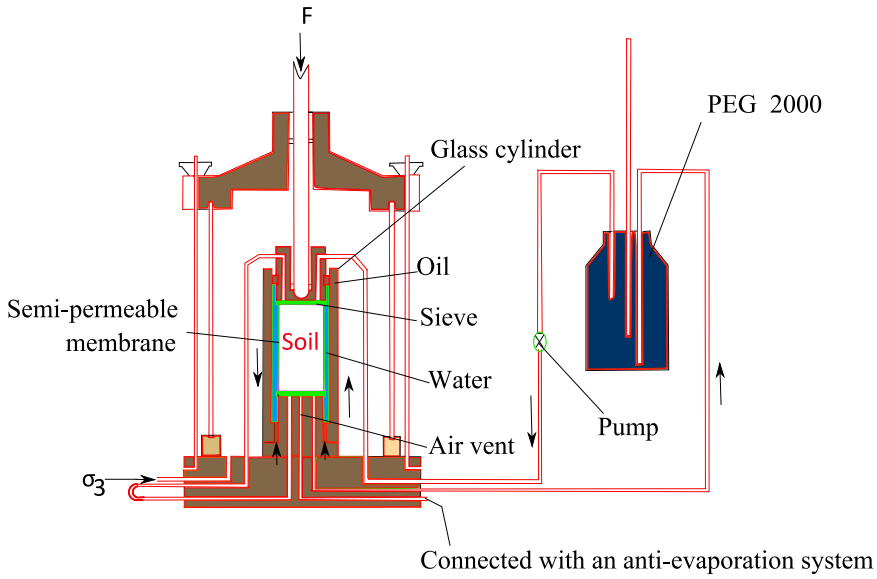

Fig. 6.13 Modified triaxial set-up using osmotic technique for unsaturated soils (after Ng and Chen, 2005, 2006)

The advantage of osmotic method to control matric suction is that the pore air can be at equilibrium with the atmosphere which simulates soil condition in the field. As discussed before, the maximum applied suction is limited by the performance of semi-permeable membrane. Further, it requires scrupulous calibration of the osmotic pressure/matric suction with different concentrations of solute using psychrometer or a osmotic pressure cell. It has been recently observed that the maximum matric suction that can be controlled by osmotic techniques is equal to the air-entry suction value. Therefore, the test results are limited by the air-entry value of the soil in this method.

Lecture 4

Measurement of the shear strength (Continued)

Extended shear box apparatus

Shear box is a simple testing apparatus to measure the shear strength of the soil in less time. The test duration is relatively small due to the smaller drainage path lengths. Fig 6.14 shows schematic diagram of the modified form of a conventional shear box apparatus for testing shear strength of unsaturated soils. The soil sample is contained in a conventional split box which allows a pre-defined failure plane along the horizontal direction. Similar to the modified triaxial apparatus using axis-translation technique, the soil sample is sandwiched between coarser porous disk and HAE discs for controlling the matric suction. The HAE disc beneath the soil sample is connected to water compartment. The pore-air and pore-water pressures are brought into equilibrium with the applied pressures. There are several transducers for application of shear force, water pressure, and air pressure; and for measurement of horizontal and vertical displacements, and water volume changes. The soil sample is initially saturated and then consolidated under a normal stress. The matric suction is increased to a required value prior to shear testing and is measured at equilibrium. Shear stress is induced along the predefined plan at a constant strain rate. Similar to the triaxial testing, shear testing is conducted under different stress state conditions using several samples. The shear test results on unsaturated decomposed granite using shear box is given in Fig 6.15 (Ng and Zhou, 2005). The results are presented as stress ratio, which is defined as the ratio of shear stress to net normal stress, and dilatancy $(\delta y/\delta x)$ against horizontal displacement, under different matric suctions.

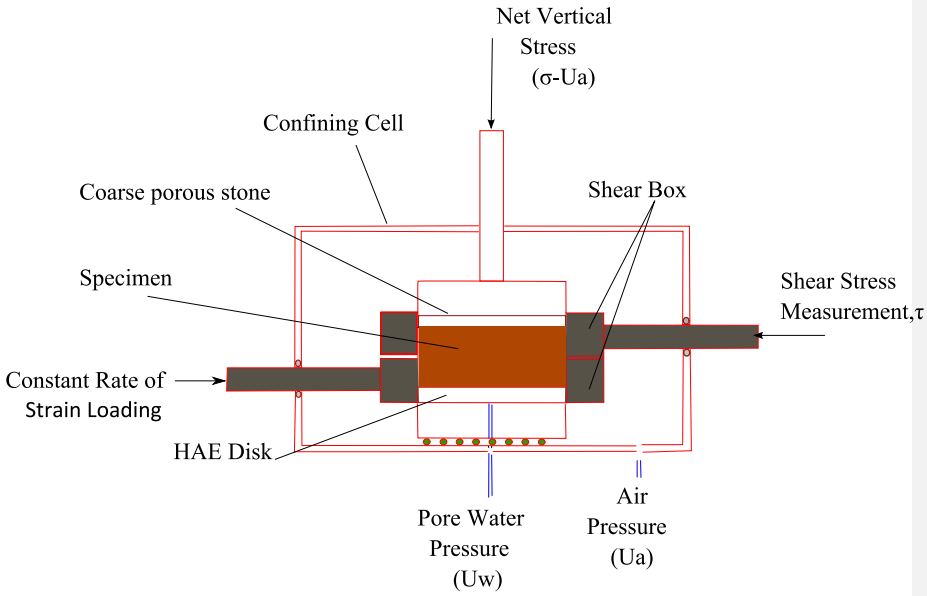

Fig. 6.14 Modified shear box apparatus for testing the strength of unsaturated soils (after Ng and Zhou, 2005)

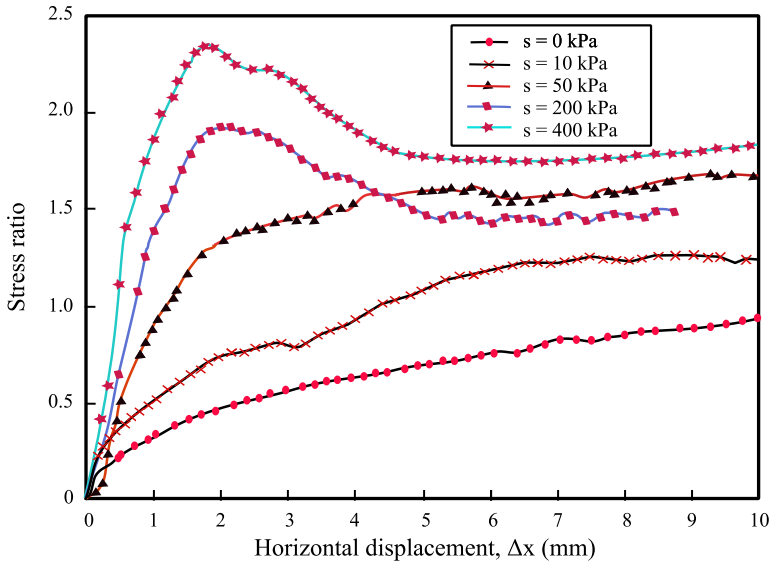

Fig. 6.15 Changes to the stress ratio during the shear under different controlled suctions (after Ng and Zhou, 2005)

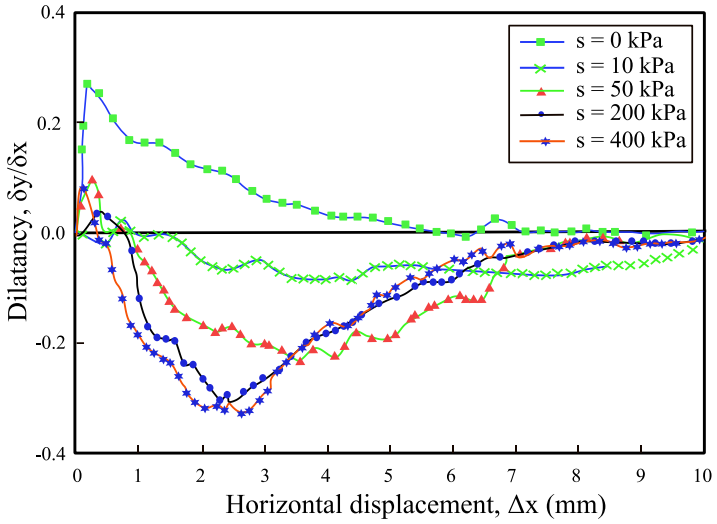

Fig. 6.16 Changes to the Dilatancy during the shear under different controlled suctions (after Lu and Likos, 2004)

It was observed that the soil displays strain-hardening behavior at lower matric suctions values. Strain softening behavior is observed with increase in the suction. Further, positive dilatancy is observed under saturation condition and an opposite behavior with matric suction value greater than zero (i.e. unsaturated soils).

Limitations associated with both axis-translation technique and conventional shear box test are applicable to the modified shear box test. Modified shear box devices using osmotic technique is also available to circumvent the limitations associated with axis-translation technique.

The laboratory shear strength test results suggest two interesting trends in the shear strength behavior as shown in Fig. 6.17 – 6.18. The shear strength of unsaturated soils increases with net normal stress. Similar trend is followed by saturated soils also. Thus, this trend can be captured even by classical M-C failure criterion by substituting unsaturated strength parameters into the equation. It is interesting to note that the failure envelopes for different matric suction or moisture contents are parallel to each other, suggesting a constant value of angle of internal friction at different matric suctions. However, the results suggest an increase in the shear strength with matric suction albeit angle of internal friction remains the same.

The shear tests are usually conducted on several identical samples by manipulating different stress state variables to obtain the strength envelope. The shear data obtained from the laboratory tests is presented in the following figures. In Fig 6.17 the data of shear strength (peak shear stress) with normal stress at different matric suction values are

provided. It can be noticed that the strength is increasing with both net normal stress and matric suction.

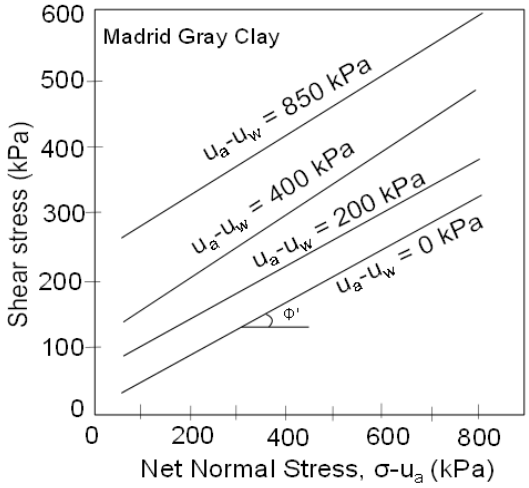

Fig. 6.17 Shear strength of Madrid Gray Clay with net normal stress under constant different matric suctions (after Escario, 1980)

Alternatively, the shear strength of Madrid Gray clay is provided against matric suction under different normal stresses in Fig 6.18. The strength is increasing with both matric suction and the normal stresses, as noticed in the previous figure. However, an interesting trend can be observed in this representation. All the strength envelopes are parallel to each other and placed one on each other in the increasing order of normal stresses. The rate of increase of shear strength with matric suction, which is represented by ϕ_b , is same under different normal stresses.

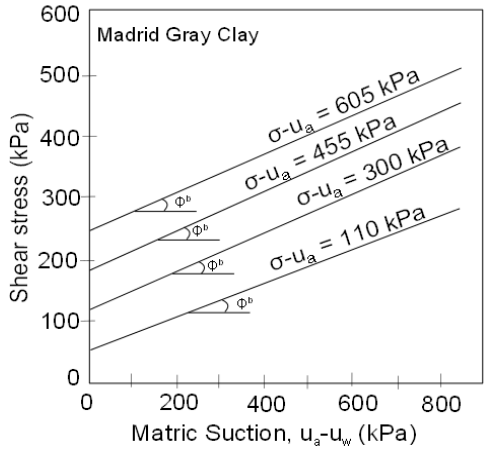

Fig. 6.18 Shear strength of Madrid Gray Clay with matric suctions under controlled net normal stress (after Escario, 1980)

Lecture 5

Measurement of Bishop's effective stress parameter

As it was mentioned earlier, Bishop (1959) was the first one to suggest two independent stress state variables viz. net normal stress and matric suction. He proposed an expression for shear strength in terms of these two independent stress state variables and a material constant, χ_f in a lumped form. The effective stress parameter χ_f is a function of negative pore water pressure or volumetric water content of the soil. However, controlling or defining this parameter is not possible. Therefore, Bishop had proposed an indirect procedure to obtain effective stress parameter, by the use of traditional M-C criterion. The traditional M-C criterion, after substituting Bishop's effective stress definition for unsaturated soils, is given by

$$\tau_f = c' + \left[(\sigma - u_a)_f + \chi_f (u_a - u_w)_f \right] \tan\phi' \qquad (6.5)$$

where τ_f is the shear strength of the unsaturated soil; and c' and ϕ' are the effective cohesion and internal friction at full saturation.

The normal stresses and matric suction are known in a modified triaxial shear test. Thus, the M-C criterion can be written in terms of principle stresses using the geometrical analysis of the following Mohr's circle as

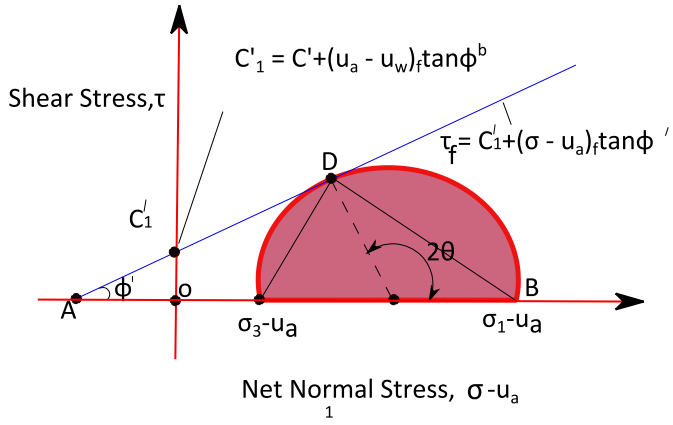

1

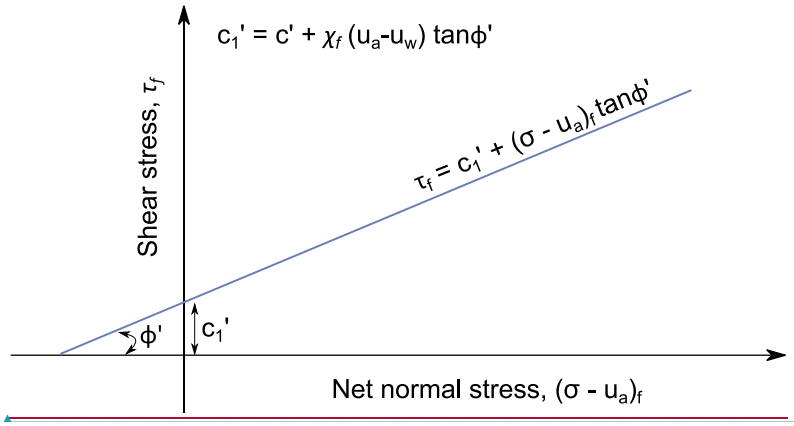

Fig. 6.19 M-C criterion for unsaturate by Bishop's approach

$$(\sigma_1 - u_a)_f = (\sigma_3 - u_a)_f \tan^2\left(\frac{\pi}{4} + \frac{\phi'}{2}\right) + 2c_1' \tan\left(\frac{\pi}{4} + \frac{\phi'}{2}\right) \quad (6.6)$$

where $c_1' = c' + \chi_f (u_a - u_w)\tan\phi'$ (6.7)

Rearranging the above equations for χ_f,

$$\chi_f = \frac{(\sigma_1 - u_a)_f - (\sigma_3 - u_a)_f \tan^2\left(\frac{\pi}{4} + \frac{\phi'}{2}\right) - 2c' \tan\left(\frac{\pi}{4} + \frac{\phi'}{2}\right)}{2(u_a - u_w)\tan\left(\frac{\pi}{4} + \frac{\phi'}{2}\right)\tan\phi'} \quad (6.8)$$

Similarly, the following equation can be used for obtaining χ_f from the extended direct shear test data

$$\chi_f = \frac{\tau_f - c' - (\sigma - u_a)\tan\phi'}{(u_a - u_w)_f \tan\phi'} \quad (6.9)$$

A relationship between effective stress parameter and degree of saturation can be established if the matric suction at failure can be used to obtain the degree of saturation from SWCC data. Based on the experimental data, it is found that the observed trend between χ_f and the degree of saturation follows $\chi_f = \left(\frac{u_a - u_w}{u_e}\right)^{-0.55}$.

Question – 6.1 A series of shear tests and water retention tests are conducted on unsaturated silty soil using modified direct shear set-up. The results are tabulated in the

Formatted: Font: 12 pt, Font color: Text 1, Complex Script Font: 12 pt

following table. Determine the shear strength parameters using Bishop's formulation and obtain a relation between the effective stress parameter and the degree of saturation.

#	u_a-u_w ψ (kPa)	Θ	$(\sigma$-$u_a)$	τ (kPa)
1	0	1	300	294
2	0	1	120	136
3	25	0.95	120	156
4	50	0.84	120	172
5	100	0.57	120	180
6	200	0.27	120	185
7	400	0.11	120	188
8	500	0.086	120	190
9	750	0.057	120	185

Solution: The cohesion intercept and friction angle under saturated condition can be obtained from the first two tests given in the table. The calculated values are c' = 30.7 kPa and $\phi' = 41.3^0$. These values can be substituted in the **Eq. # 6.9** for obtaining effective stress parameter under different matric suction as tabulated in the following table. z

Table. Computed effective stress parameter

#	u_a-u_w (kPa)	Θ	$(\sigma$-$u_a)_f$	τ_f (kPa)	χ_f
1	0	1	300	294	1
2	0	1	120	136	1
3	25	0.95	120	156	.905
4	50	0.84	120	172	0.817
5	100	0.57	120	180	0.50
6	200	0.27	120	185	0.278
7	400	0.11	120	188	0.148
8	500	0.086	120	190	0.123
9	750	0.057	120	185	0.0741

The SWCC and the relation between effective stress parameter and the degree of saturation are established and shown in the following figures.

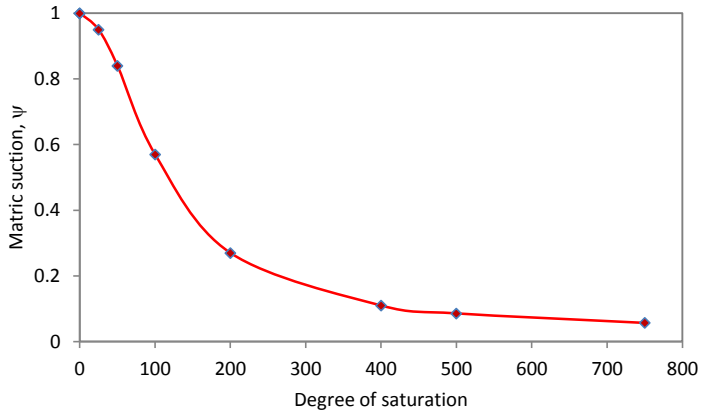

Fig. 6.21 SWCC for the example problem

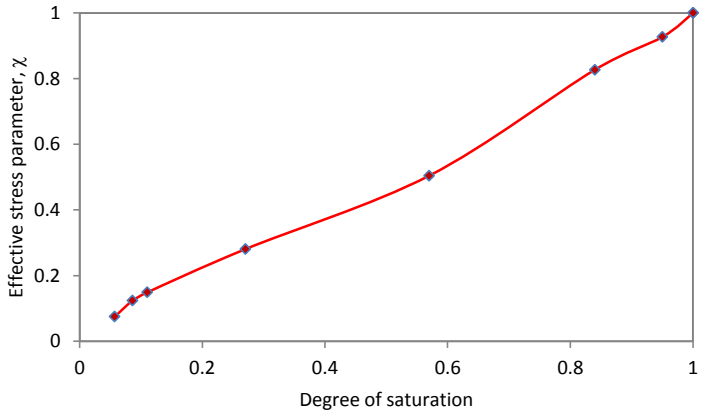

Fig. 6.22 Relation between effective stress parameter with degree of saturation for the example problem – 6.1

Question – 6.2 A series of shear tests and water retention tests are conducted on unsaturated sand using modified triaxial set-up. The results are tabulated in the following table. Determine the shear strength parameters using Bishop's formulation and obtain a relation between the effective stress parameter and the degree of saturation.

#	u_a-u_w (kPa)	$(\sigma_1$-$u_a)_f$	$(\sigma_3$-$u_a)_f$
1	0	180	50
2	10	200	50
3	25	220	50
4	50	230	50
5	100	240	50
6	200	250	50
7	400	265	50
8	500	280	50
9	750	300	50

Solution: The strength parameters under saturated condition can be obtained from a single test as the cohesion intercept is zero (sandy soil). The friction angle can be obtained from the Mohr's circle,

$$\phi' = \sin^{-1}\left(\frac{\sigma_1 - \sigma_3}{\sigma_1 + \sigma_3}\right) = 34.41^0.$$

Assuming that the saturated strength parameters are valid at any degree of saturation, the Eq # 6.8 is used to obtain the effective stress parameter under various degree of saturation. The computed data is tabulated below

#	u_a-u_w (kPa)	$(\sigma_1 u_a)$	$(\sigma_2$-$u_a)$	χ_f
1	0	180	50	1
2	10	200	50	0.772
3	25	220	50	0.617
4	50	230	50	0.385
5	100	240	50	0.231
6	200	250	50	0.135
7	400	265	50	0.0818
8	500	280	50	0.077
9	750	300	50	0.0616

The relationship between matric suction and effective stress parameter is presented in the Fig. 6.23.

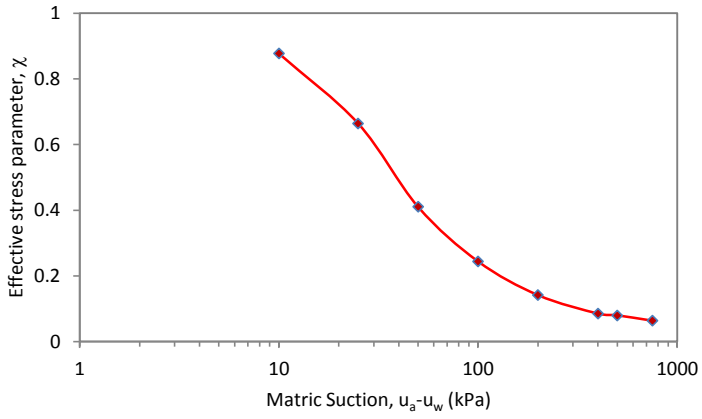

Fig. 6.23 Relation between effective stress parameter with degree of saturation for the example problem 6.2

Lecture 6

Extended M-C criterion by Fredlund

Null tests for stress state variables

Null tests are important in understanding the extended M-C failure criterion as they prove the validity of the hypothesis for stress state variables. It is based on the manipulation of different combinations of stress variables. Either change to the total volume of the specimen or changes in the degree of saturation should be negligible under the correct/valid combination of stress state variables. Matric suction and net normal stresses can conveniently be controlled in the extended shear tests by manipulating the pore-air, pore-water, and confining pressures in the tests. Fredlund and Morgenstern conducted 19 null-type tests in 1977 by manipulating pore-air, pore-water, and confining pressures in several tests on compacted kaolinite specimens to identify the stress state variables of unsaturated soils using modified consolidation and triaxial test set-ups. The influence of these variables on the macroscopic behavior of these soils is evaluated under different stress states. The following table, Table 6.1, presents some data of pressure changes from the null tests on unsaturated soil samples.

Table 6.1 Pressure changes in Null-type tests (*Source*: Fredlund and Rahardjo, 1993)

Test number	Initial stresses (kPa)			Changes in Stresses (kPa)		
	Total stress, σ	Pore-air pressure, u_a	Pore-water pressure, u_w	$\Delta\sigma$	Δu_a	Δu_w
23	420.7	278.7	109.6	+71.4	+70.3	+70.7
25	495.3	406.8	143.5	+68.6	+68.3	+66.9
27	234.2	138.3	100.3	+68.8	+68.5	+80.8
29	274.6	202.2	22.4	+68.5	+68.3	+68.8
31	411.4	338.3	160.2	+68.1	+68.0	+67.3
33	549.0	476.4	297.2	+69.0	+68.0	+68.4
35	410.9	338.5	208.3	+69.5	+69.3	+69.7
37	547.5	473.7	343.9	+67.9	+67.5	+67.4
39	549.4	477.1	347.6	-70.2	-69.5	-69.8
41	412.6	340.7	211.4	-140.5	-140.3	-139.8

The stress variables are varied in the experiments according to

$$\Delta\sigma_x = \Delta\sigma_y = \Delta\sigma_z = \Delta u_w = \Delta u_a$$

so that the values for stress state variables viz. $(\sigma - u_a)$, $(\sigma - u_w)$, and $(u_a - u_w)$ are maintained constant. The changes in the volume of overall specimens are less than the 0.4% of the original volume. The overall volume of the soil sample and the degree of saturation remained constant throughout the "null" experiments reflecting the applicability

of the proposed variables to be the stress state variables. Further tests by other researchers also supported this premise. Thus, any two of three stress variables, $(\sigma - u_a)$, $(\sigma - u_w)$, and $(u_a - u_w)$, may be considered as stress state variables. The following table provides the test conditions to verify this combination.

Table 6.2 Independent stress state variables controlled in the tests (*Source*: Bishop and Donald, 1961)

#	Group – 1		Group – 2		Group – 3	
	$\sigma_3 - u_a$ kPa	$u_a - u_w$ kPa	$\sigma_3 - u_w$ kPa	$u_a - u_w$ kPa	$\sigma_3 - u_a$ kPa	$\sigma_3 - u_w$ kPa
1	44.8-31.0 = 13.8	31.0-(-27.6) = 58.6	72.4	58.6	13.8	72.4
2	77.2-63.4 = 13.8	63.4-(+4.8) = 58.6	72.4	58.6	13.8	72.4
3	13.8-0.0 = 13.8	0-(-58.6) = 58.6	72.4	58.6	13.8	72.4
4	110.3-96.5 = 13.8	96.5-(+37.9) = 58.6	72.4	58.6	13.8	72.4

The combination of these stress state variables, in the tests did not produce any significant changes in the shear strength of the soils. Any of these two stress state variables, thus, control the strength of the unsaturated soils.

Fredlund et al. (1978) proposed a lucid and simple M-C criterion to account for the increase in shear strength with unsaturation by introducing a new variable ϕ^b. The extended M-C criterion can be written in terms of the two stress state variables as

$$\tau_f = c'_{\psi_m=0} + (\sigma - u_a)_f \tan\phi' + (u_a - u_w)_f \tan\phi^b \qquad (6.10)$$

where $c'_{\psi_m=0}$ is the cohesion intercept of saturated system and at zero net normal stress; and ϕ^b the internal friction angle associated with matric suction. The extended M-C criterion is expressed as a three-dimensional surface in an extended matric suction axis. The failure envelope described in Eq 6.10 is a planar surface created by the stress state variables τ, $(\sigma - u_a)$, and $(u_a - u_w)$. The internal friction angle in the third term on the right-hand side of equation describes the rate of increase in shear strength relative to the matric suction on the τ vs. $(u_a - u_w)$ plane. The other two terms express the conventional M-C criterion. The failure surface based on extended M-C criterion is illustrated in the Fig 6.24.

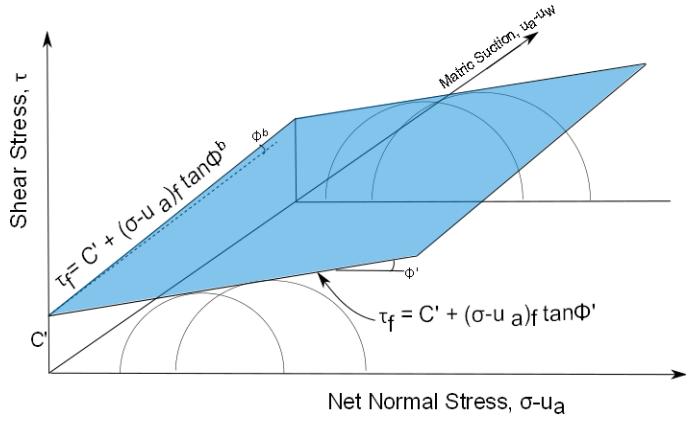

Fig. 6.24 Extended M-C criterion

It appears from the figure that ϕ^b is smaller than ϕ'. Fredlund et al. (2012) showed on several soils that ϕ^b is either smaller or equal to ϕ'.

Lecture 7

Estimation of extended M-C parameters

Question – 6.3. Triaxial testing on clay soil is conducted using modified triaxial testing machine. The sample is in equilibrium under the all-round pressure of 300 kPa, deviator stress of 100 kPa, pore-air pressure of 200 kPa, and pore water pressure of 100 kPa. Illustrate the state of stress using Mohr's circle and find the maximum shear stress.

Solution: As we discussed earlier, the state variables need to be defined in unsaturated soils for defining the stress state. The two state variables viz. net normal and matric suction for the present problem are computed here for the representation of stresses.

The minor principle stress is equal to all-round pressure in this case. Thus, $\sigma_3 = 300$ kPa.

Major principle stress $\sigma_1 = \sigma_3 + \Delta\sigma$ = 300 + 100 = 400 kPa.

Net normal stresses: $\sigma_1 - u_a = 400 - 200 = 200$ kPa and $\sigma_3 - u_a = 300 - 200 = 100$ kPa

matric suction $u_a - u_w = 200 - 100 = 100$ kPa

The Mohr circle for the state of stress is shown in the following figure

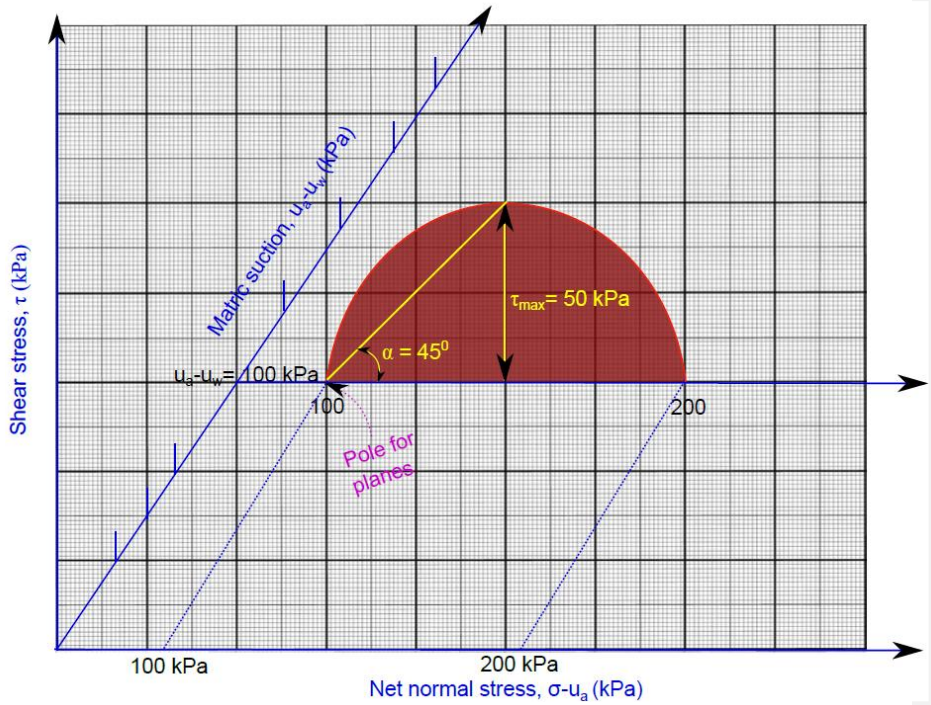

Fig. 6.25 Mohr's circle representation of the stresses for problem 6.3

As shown in the figure, the maximum shear stress is equal to the half the diameter of Mohr's circle which is equal to 50 kPa. The angle at which the maximum shear stress acts with respect to the major principle stress is found by drawing a line from the pole for planes to the maximum shear stress point. This angle is equal to 45^0.

Question – 6.4. Analyze the state of stress at a point, *A*, located few meters below the ground surface, in front of the civil engineering building of IIT Guwahati, Assam. The vertical normal stress at *A* is 400 kPa, and other principle stresses are 100 kPa and 50 kPa, respectively. The pore water pressure is expected to vary from -250 kPa to -50 kPa during the months of January and May. The principle stresses are estimated to decrease 10% in the month of May. Assume the pore air pressure to be at a zero reference value.

Solution: The net normal stresses at point *A* are

in January: $\sigma_1 - u_a = 400$ kPa, and $\sigma_2 - u_a = 100$, and $\sigma_3 - u_a = 50$ kPa.

in May: $\sigma_1 - u_a = 360$ kPa, and $\sigma_2 - u_a = 90$, and $\sigma_3 - u_a = 45$ kPa.

The matric suction is $u_a - u_w = 250$ kPa in the month of January and 50 kPa in the May. The state of stresses are given by drawing the Mohr's circle for the present stress state in the following figure.

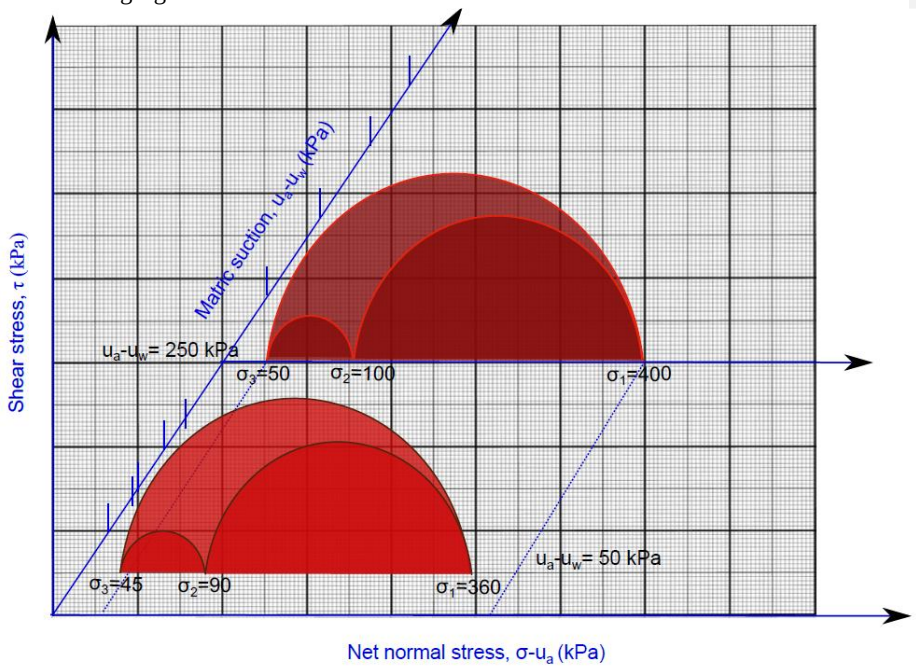

Fig. 6.26 Mohr's circle representation of the state of stresses for problem 6.4

Lecture 8

Estimation of extended M-C parameters (Continued)

Question – 6.5. A series of shear tests are conducted on the extended triaxial apparatus on four identically prepared samples of unsaturated clay. The state of stresses developed in the soil at failure for all the four tests are given below.

Test 1: $\sigma_1 - u_a = 60$ kPa, $\sigma_2 - u_a = \sigma_3 - u_a = 10$ kPa and $u_a - u_w = 0$ kPa

Test 2: $\sigma_1 - u_a = 100$ kPa, $\sigma_2 - u_a = \sigma_3 - u_a = 30$ kPa and $u_a - u_w = 0$ kPa

Test 3: $\sigma_1 - u_a = 100$ kPa, $\sigma_2 - u_a = \sigma_3 - u_a = 10$ kPa and $u_a - u_w = 60$ kPa

Test 4: $\sigma_1 - u_a = 142$ kPa, $\sigma_2 - u_a = \sigma_3 - u_a = 30$ kPa and $u_a - u_w = 60$ kPa

Find the unsaturated shear strength parameters using extended M-C criterion.

The state of stress in the soils during the first two tests ($u_a - u_w = 0$) is represented by Mohr's circle as shown in Fig. 6.27. The material constant ϕ' and c_1' can be obtained using line joining the two circles.

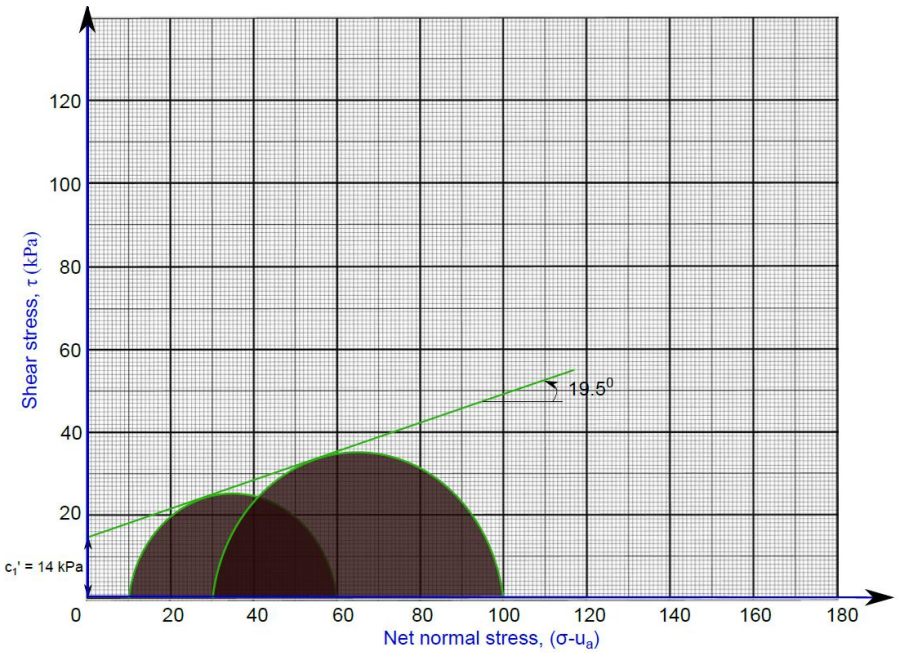

Fig. 6.27 Mohr's circle representation of the state of stresses for problem 6.5 from tests – 1&2

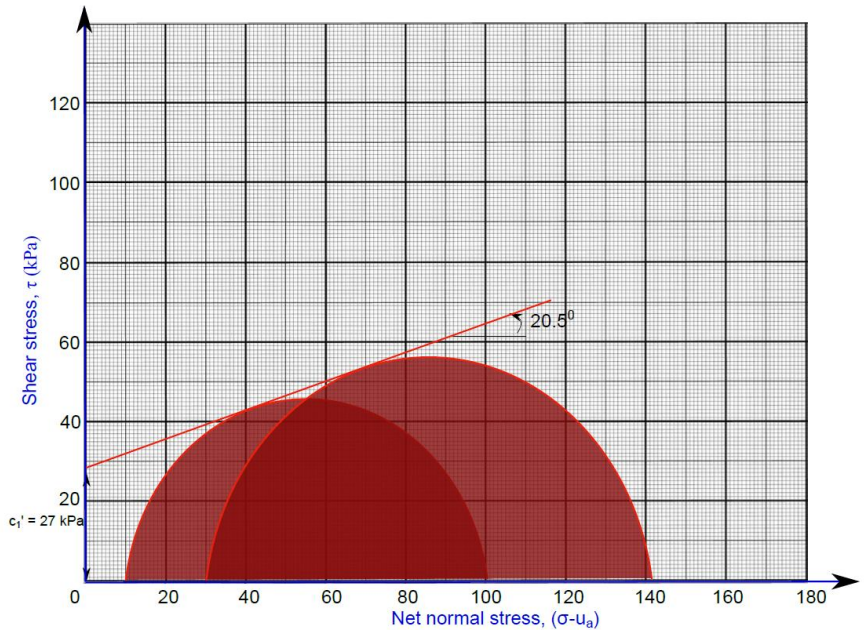

Fig. 6.28 Mohr's circle representation of the state of stresses for problem 6.5 from tests – 3&4

Similarly, the material constant ϕ' and c_2' are obtained using tests 3 & 4 as shown in Fig. 6.28. The ϕ' values obtained from both the test series are similar as noted by experimental observations by Escario (1980). Therefore, an average value can be used to represent the angle of internal friction of the soil. Fig. 6.29 shows the graphical representation of the state of stresses in soils during all the four tests. The ϕ^b can be obtained by plotting the data of c_1', c_2', and ϕ' on shear stress – matric suction plane as shown in Fig. 6.30. The stress representation and extended M-C failure surface for the problem 6.5 are given in Fig. 6.31.

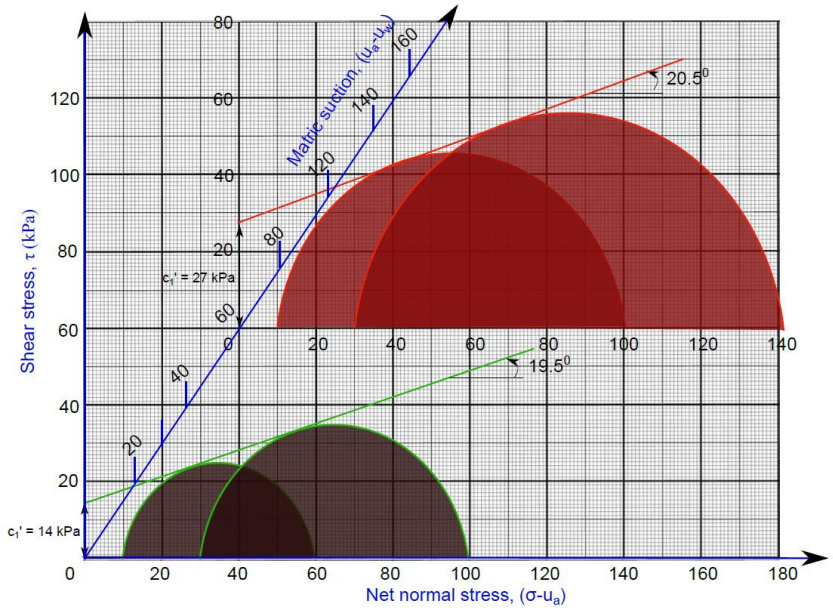

Fig. 6.29 Mohr's circle representation of the state of stresses for problem 6.5 from all the tests

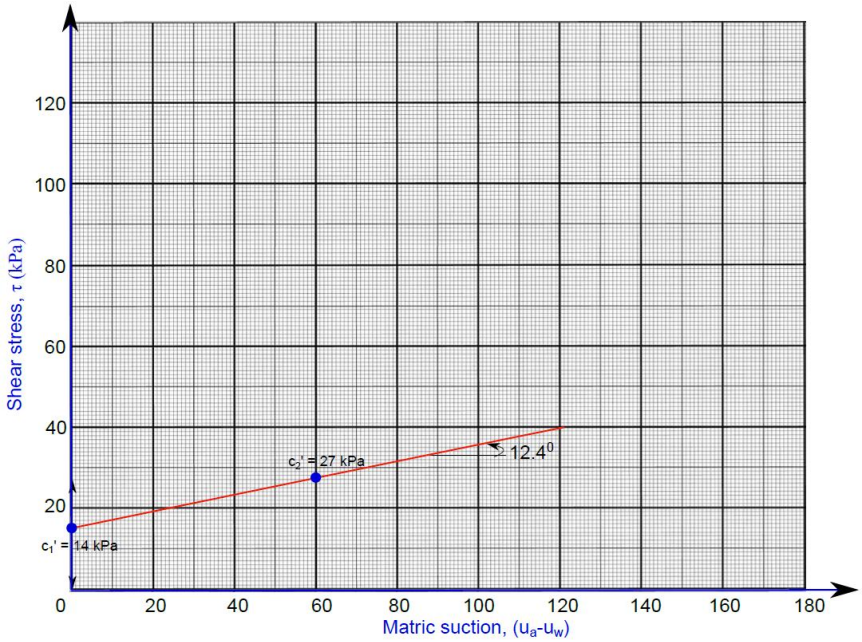

Fig. 6.30 Mohr's circle representation of the state of stresses for problem 6.5

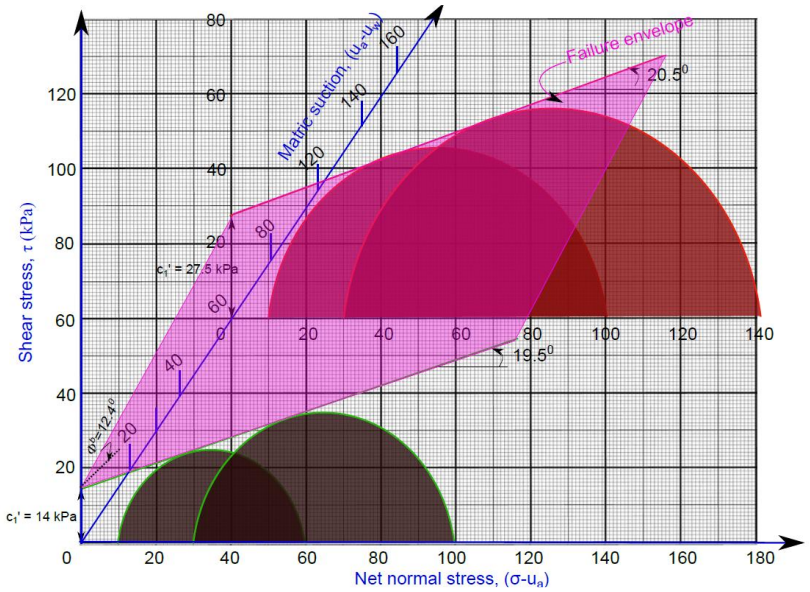

Fig. 6.31 Mohr's circle representation of the state of stresses and failure surface for problem 6.5

Lecture 9

Estimation of extended M-C parameters (Continued)

Question – 6.6. A series of shear tests are conducted on the extended triaxial apparatus on four identically prepared samples of unsaturated clay. The state of stresses developed in the soil at failure for all the four tests are given below.

Test 1: $\sigma_1 - u_a = 100$ kPa, $\sigma_2 - u_a = \sigma_3 - u_a = 30$ kPa and $u_a - u_w = 40$ kPa

Test 2: $\sigma_1 - u_a = 200$ kPa, $\sigma_2 - u_a = \sigma_3 - u_a = 80$ kPa and $u_a - u_w = 40$ kPa

Test 3: $\sigma_1 - u_a = 180$ kPa, $\sigma_2 - u_a = \sigma_3 - u_a = 30$ kPa and $u_a - u_w = 120$ kPa

Test 4: $\sigma_1 - u_a = 280$ kPa, $\sigma_2 - u_a = \sigma_3 - u_a = 80$ kPa and $u_a - u_w = 120$ kPa

Find the unsaturated shear strength parameters using extended M-C criterion.

The state of stress in the soils during the first two tests ($u_a - u_w = 40$) is represented by Mohr's circle as shown in Fig. 6.32. The material constant ϕ' and c_1' can be obtained using line joining the two circles.

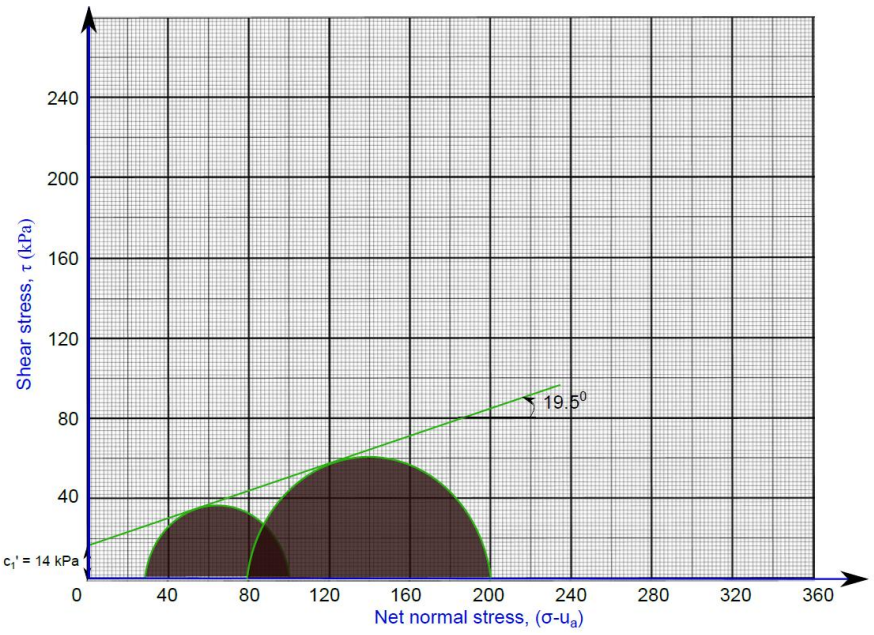

Fig. 6.32 Mohr's circle representation of the state of stresses for problem 6.6 from tests – 1&2

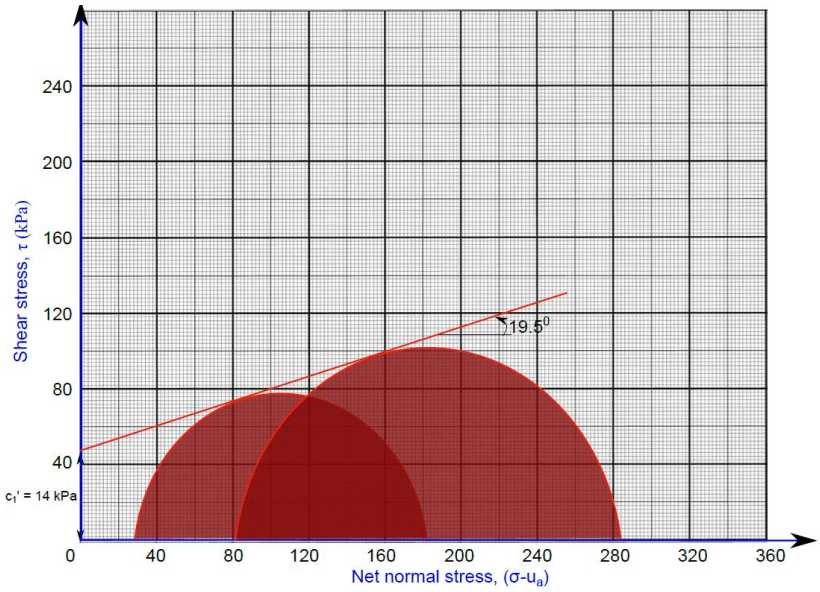

Fig. 6.33 Mohr's circle representation of the state of stresses for problem 6.6 from tests – 3&4

Similarly, the material constant ϕ' and c_2' are obtained using tests 3 & 4 as shown in Fig. 6.33. An average value can be used to represent the angle of internal friction of the soil. Fig. 6.34 shows the graphical representation of the state of stresses in soils during all the four tests. The ϕ^b can be obtained by plotting the data of c_1', c_2', and ϕ' on shear stress – matric suction plane as shown in Fig. 6.35. The stress representation and extended M-C failure surface for the problem 6.5 are given in Fig. 6.36.

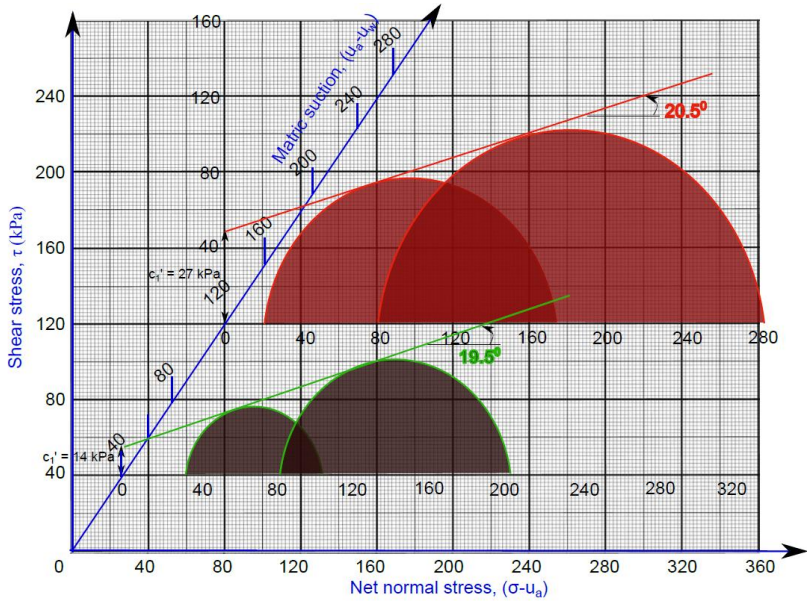

Fig. 6.34 Mohr's circle representation of the state of stresses for problem 6.6 from all the test data

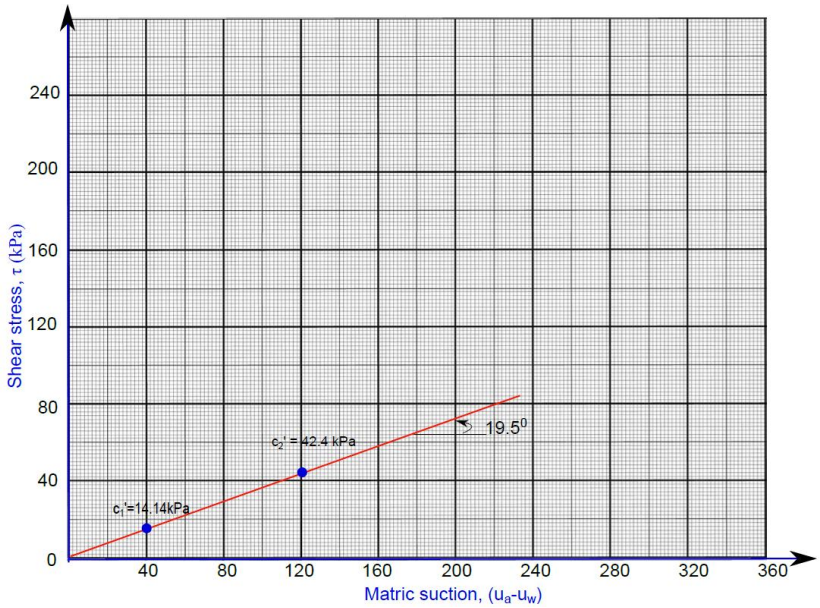

Fig. 6.35 Strength envelope for problem #6.6

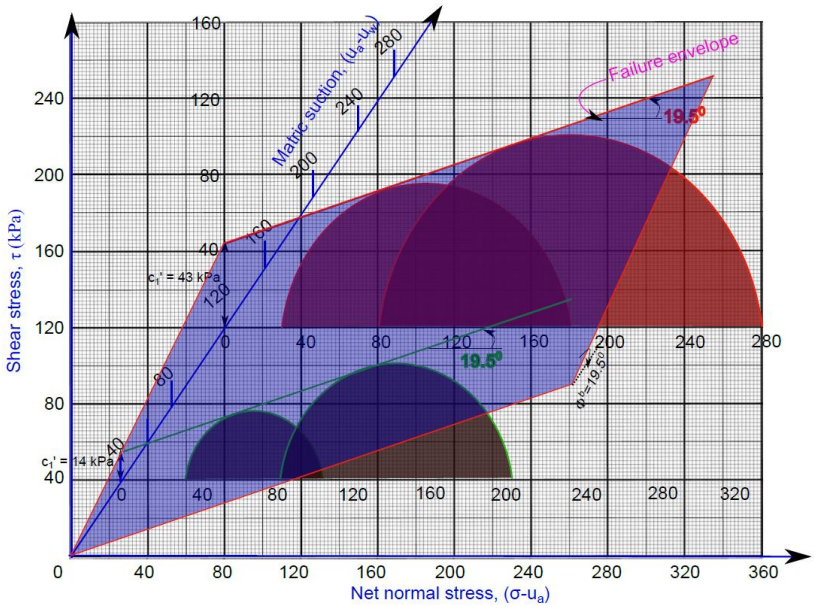

Fig. 6.36 Modified M-C envelope and failure surface for the problem #6.6

Lecture 10

Estimation of extended M-C parameters (Continued)

Question – 6.7. A series of shear tests are conducted on the extended direct shear apparatus on four identically prepared samples of unsaturated clay. The state of stresses developed in the soil at failure for all the four tests are given below.

Test 1: $u_a - u_w = 10$ kPa, $(\sigma - u_a)_f = 100$ kPa, and $\tau_f = 55$ kPa

Test 2: $u_a - u_w = 10$ KPa, $(\sigma - u_a)_f = 300$ kPa, and $\tau_f = 150$ kPa

Test 3: $u_a - u_w = 300$ kPa, $(\sigma - u_a)_f = 170$ kPa, and $\tau_f = 240$ kPa

Test 4: $u_a - u_w = 300$ kPa, $(\sigma - u_a)_f = 295$ kPa, and $\tau_f = 300$ kPa

Find the unsaturated shear strength parameters using extended M-C criterion.

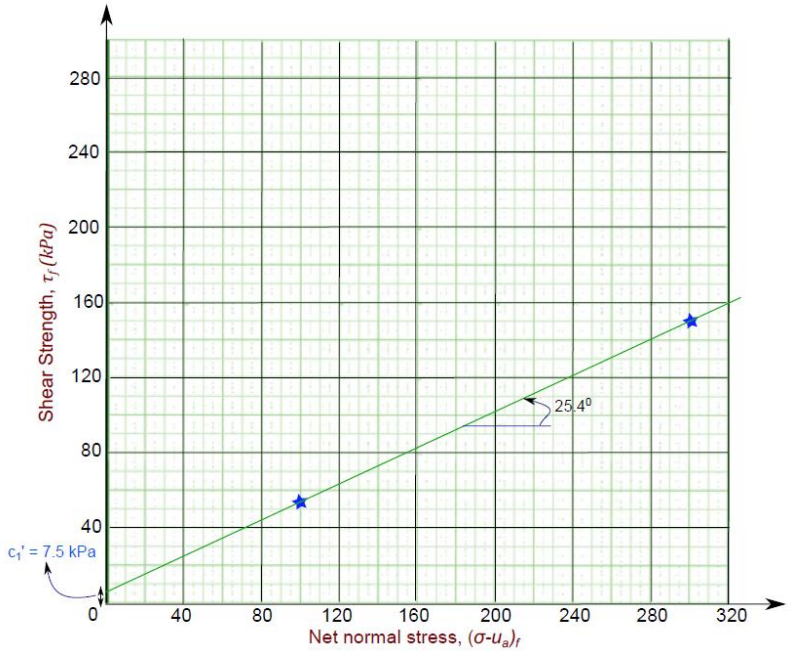

Fig. 6.37 Strength envelope for matric suction of 10 kPa

The state of stress in the soils during the first two tests is represented by Mohr's circle as shown in Fig. 6.37. The material constant ϕ' and c_1' can be obtained using line joining the two circles. Similarly, the material constant ϕ' and c_2' are obtained using tests 3 & 4 as shown in Fig. 6.38. An average value can be used to represent the angle of internal friction of the soil. Fig. 6.39 shows the graphical representation of the state of stresses in

soils during all the four tests. The stress representation and extended M-C failure surface for the problem 6.5 are given in Fig. 6.40.

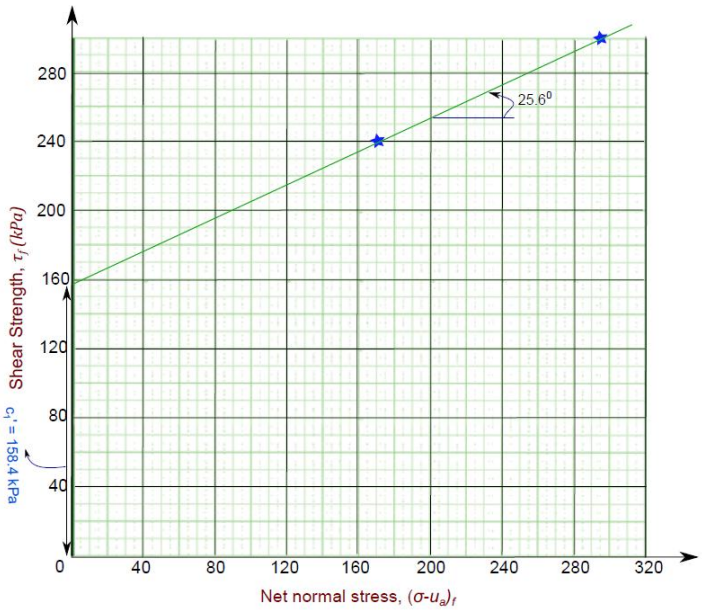

Fig. 6.38 Strength envelope for matric suction of 300 kPa

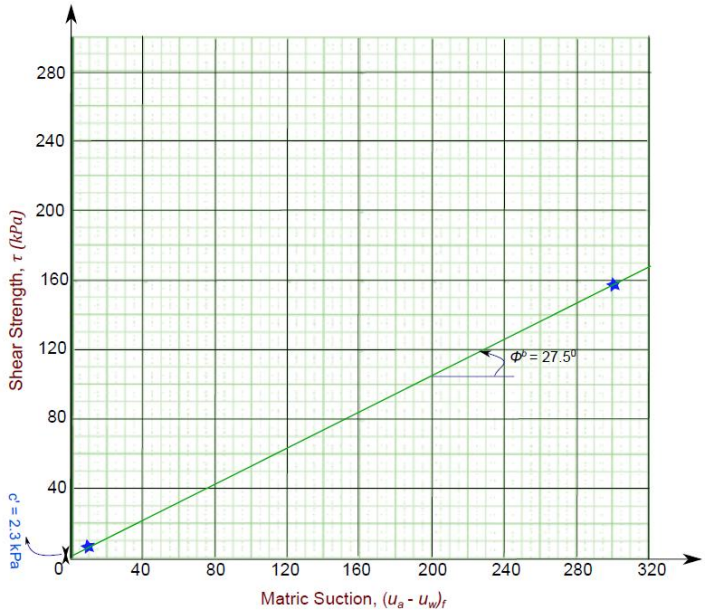

Fig. 6.39 Strength envelope for problem #6.7

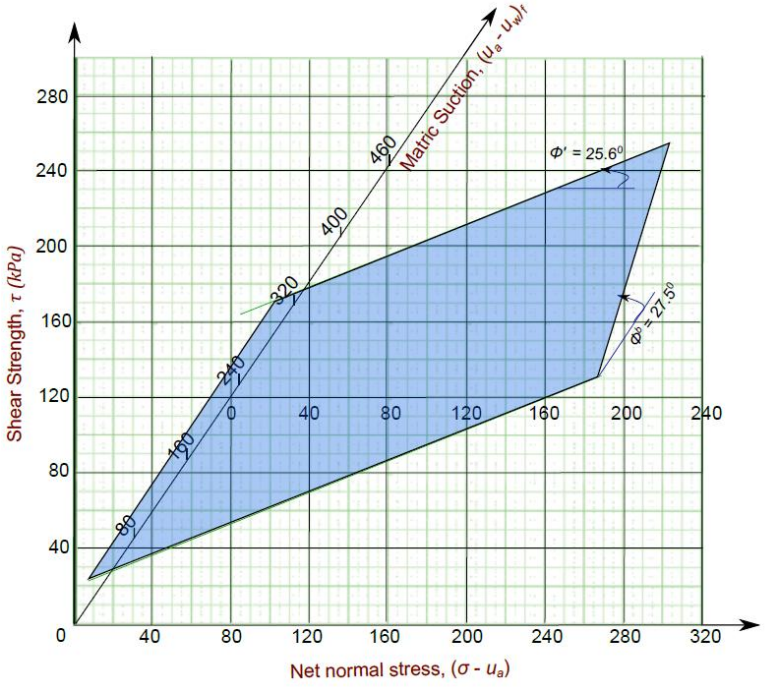

Fig. 6.40 Modified M-C envelope for problem #6.7

Lecture 11

Nonlinearity in the extended M-C failure envelope

The extended M-C theory to explain the variation of shear strength with matric suction received a wide spread recognition due to its simplicity. However, the applicability of the theory over a wide range of matric suctions is questionable. This particular aspect limits the generality of the theory. Recent experimental data showed that the variable, ϕ^b, describing the dependency of strength on matric suction is highly nonlinear. The variable can vary nonlinearly from ϕ' in the saturated portion of SWCC to zero near the residual saturation portion of SWCC. Sometimes it was also observed the variable reached below zero for suctions approaching the residual saturation state. The following figures, Fig. 6.41 – 6.42, illustrates the nonlinear nature of ϕ^b observed in the experiments over a wide range of matric suctions using modified direct shear tests on unsaturated glacial till and clays, respectively.

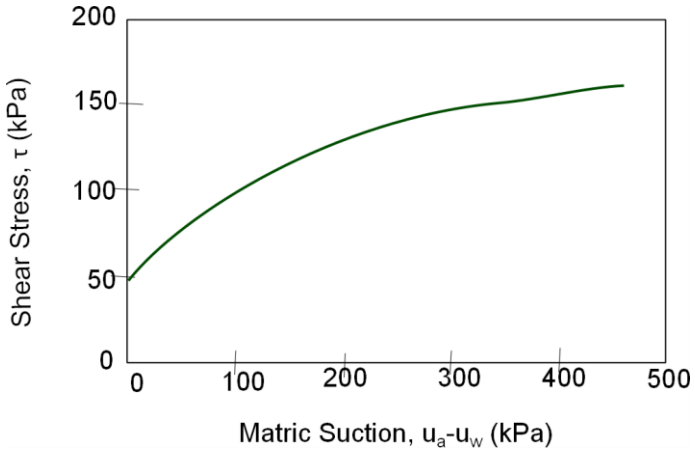

Fig. 6.41 Dependency of shear strength on matric suction (after Gan et al., 1988)

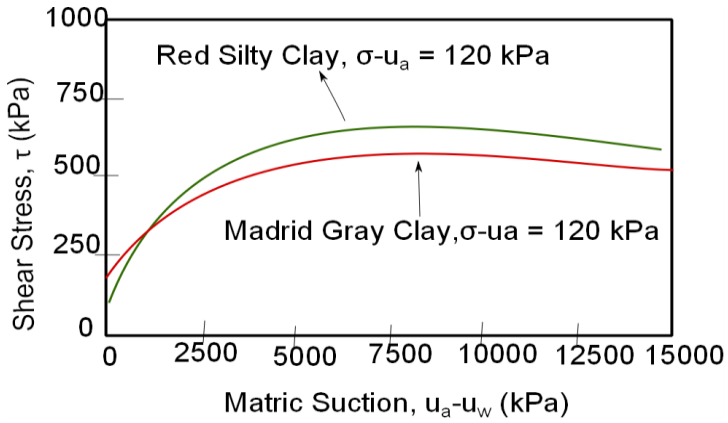

Fig. 6.42 Dependency of shear strength on matric suction for two different clays (after Escario et al., 1989)

Fig. 6.42 shows the shear strength (peak shear stress) as a function of matric suction. The experimental data suggests a decrease in ϕ^b with matric suction in both Red Silty Clay and Madrid Gray Clay. The variable becomes negative for clayey soils after reaching the matric suction value of around 7500 kPa. The shear strength analysis in such cases can be handled by considering several linear segments of strength envelope with varying ϕ^b angles beyond the air-entry pressure. However, the envelope may be approximated by assuming ϕ^b to be equal to ϕ' in the initial regime, starting from the saturation to air-entry pressure. The entire non-linear regime can also be approximated (Fredlund et al. 1987) by linear curve by a conservative approach.

Lecture 12

Empirical relations for predicting shear strength

It appears from the non-linear nature of the variable ϕ^b that the variable ϕ^b is related to the slope of SWCC curve. Vanapalli et. al. (1996) had provided a conceptual relationship between nonlinear nature of the shear strength for increasing matric suction to the drying SWCC as shown in Fig. 6.43 for a typical soil.

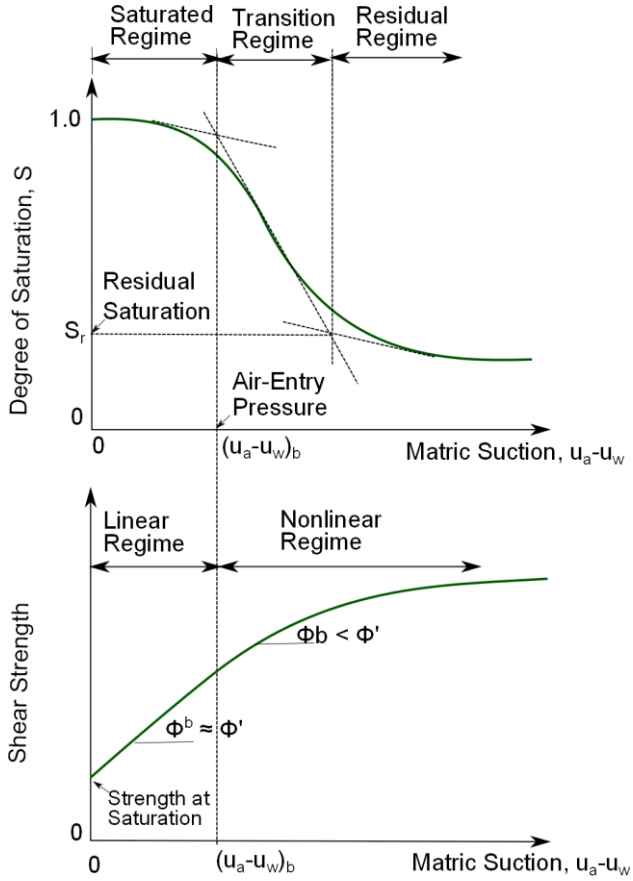

Fig. 6.43 Conceptual comparison of SWCC against the increase strength with matric suction (after Vanapalli ct.al., 1996)

The failure envelope on the $\tau_f - \psi_m$ plane is linear and equal to the angle of internal friction, ϕ', of the soil up to the air-entry pressure as shown in the figure. The shear strength envelope is nearly linear in the saturated portion of the SWCC as the matric suction is relatively low in this region. The contribution of matric suction to the increase in the shear

strength may be handled using the conventional M-C failure envelope using a negative pore pressure value. Beyond the saturated portion of the SWCC, the shear strength envelope is nonlinear due to the unsaturation of the soil pores. The resultant inter-particle forces in the three phase system contribute to the shear strength. According to this premise, the reduction in the pore saturation effectively reduces the contribution of matric suction to the increasing shear strength. The shear strength of sands, silts, and some clays decreases beyond residual value of suction.

Shear strength and soil water characteristic curve

Vanapapplli et al. (1996) suggested an empirical approach for predicting the shear strength envelope of unsaturated soils from soil-water characteristic curve. The following empirical equation has been developed for the relation.

$$\tau = \left[c' + (\sigma - u_a)\tan\phi'\right] + (u_a - u_w)\left(\Theta^k \tan\phi'\right) \qquad (6.11)$$

where k is the fitting parameter. This is similar to the Bishop's formulation for shear strength of unsaturated soils in which χ_f is replaced with Θ^k. One can realize that the relationship between χ_f and Θ was established on experimental data in Lecture – 5. However, in this procedure, the normalized volumetric water content, Θ, is estimated using the following equation (Fredlund and Xing, 1994)

$$\Theta = \left[1 - \frac{\ln\left(1 + \frac{u_a - u_w}{C_r}\right)}{\ln\left(1 + \frac{10^6}{C_r}\right)}\right]\left[\frac{1}{\ln\left(\exp(1) + \left(\frac{u_a - u_w}{a}\right)^n\right)}\right]^m \qquad (6.12)$$

where a, m, n, and C_r are the fitting constants. The first term (half) of the right-hand side of equation, Eq. 6.11, represents the saturated shear strength when u_a is replaced with u_w. The second half of the equation is the contribution of matric suction to the shear strength which is predicted by SWCC in this equation. This eliminates the need for the modified shear tests for controlling pore-air and pore-water pressures which is necessary for the shear tests under varied matric suctions. However, it requires a reliable estimation of SWCC of the soil representing the field loading conditions. It can be obtained using pressure-plate apparatus under specified loading conditions.

Question – 6.8 Predict the unsaturated shear strength envelope from the following SWCC data obtained by axis-translation technique in the laboratory using empirical equation. The saturated shear strength parameters obtained from conventional shear testing procedure are c′ = 25 kPa, ϕ′ = 20^0, and net normal stress, $(\sigma - u_a)$, is 100 kPa.

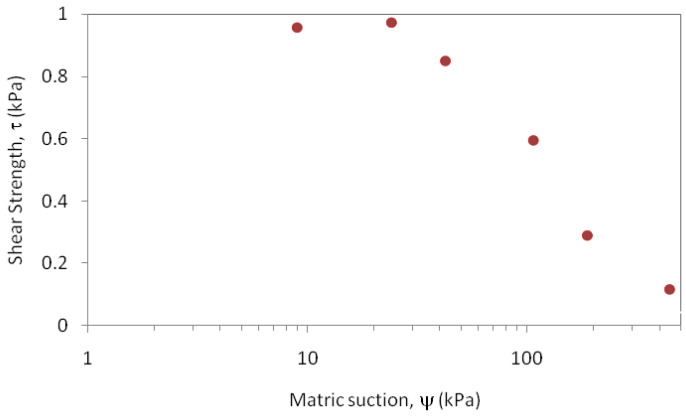

Fig. 6.44. SWCC laboratory data

Solution: The SWCC data given in the problem can be fitted with **Fredlund and Xing (1994)** model for smooth and continuous distribution of SWCC by any optimization algorithm. The theoretical fit to the given data along with the equation are shown here.

$$\Theta = \left[1 - \frac{\ln\left(1 + \frac{u_a - u_w}{1500}\right)}{\ln\left(1 + \frac{10^6}{1500}\right)}\right]\left[\frac{1}{\ln\left(\exp(1) + \left(\frac{u_a - u_w}{100}\right)^2\right)}\right]^2 \qquad (6.13)$$

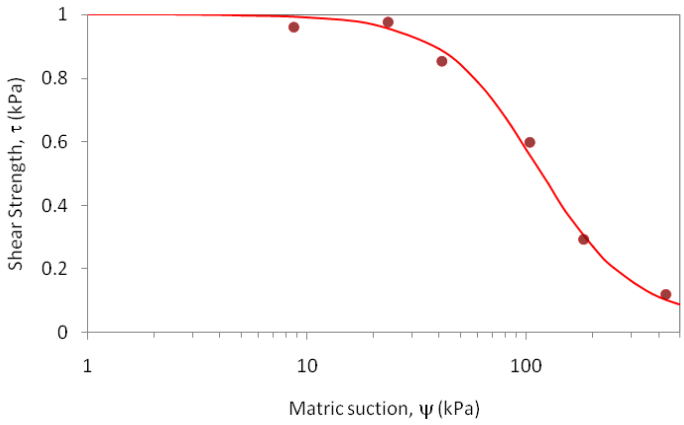

Fig. 6.45. Theoretical fit to the SWCC data

The empirical equation **Eq. 9.11** can now be used to predict the shear strength envelope at any with matric suction. However, the fitting parameter *k* is not given. It is usually obtained by fitting the theoretical strength envelope with the experimental data. Thus a value of *k* = 1 is assumed to use the empirical procedure.

Table 6.3. Shear strength calculation from SWCC

Data #	ψ (kPa)	Θ	τ (kPa)
1	1	0.999824	61.76093
2	2.5	0.999284	62.3063
3	5	0.997653	63.2126
4	10	0.991682	65.00645
5	20	0.969434	68.45392
6	40	0.891107	74.37049
7	60	0.786237	78.56703
8	80	0.675959	81.07933
9	100	0.574072	82.29153
10	125	0.467102	82.64844
11	150	0.383426	82.33036
12	200	0.270301	81.0733
13	250	0.202876	79.85722
14	400	0.112288	77.74484
15	500	0.086602	77.15733

The computed strength data with matric suction from theoretical SWCC data is tabulated below. The envelope is plotted in the Fig. 6.46. It can be observed that the strength increases up to 100 kPa and then decreases with matric suction.

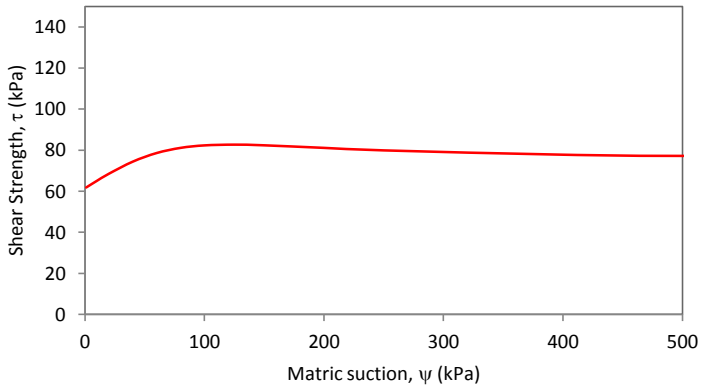

Fig. 6.46 Theoretical shear strength envelope empirically obtained from SWCC data

However, the quantitative description and accuracy of the shear strength data with matric suction using Eq. 6.12 can be ascertained only after thorough validation experiments on several soils over a wide range of matric suctions. At present, the shear tests on unsaturated soils over a wide range of matric suctions are not available currently.